THIS REPORT HAS BEEN DECLASSIFIED
AND CLEARED FOR PUBLIC RELEASE.

DISTRIBUTION A
APPROVED FOR PUBLIC RELEASE;
DISTRIBUTION UNLIMITED.

BEAM ANALYZER

3. Beam Analysis With a Circularly Deflecting System

N6-ori-71 Task XIX
NR 073 162

TECHNICAL REPORT No. 5-3

ELECTRICAL ENGINEERING RESEARCH LABORATORY
ENGINEERING EXPERIMENT STATION
UNIVERSITY OF ILLINOIS
URBANA, ILLINOIS

BEAM ANALYZER

3. BEAM ANALYSIS IN A CIRCULARLY DEFLECTING SYSTEM

N6-ori-71　　　Task XIX
Technical Report No. 5-3
NR 073 162

Date:

January 1953

ELECTRON TUBE SECTION
ELECTRICAL ENGINEERING RESEARCH LABORATORY
ENGINEERING EXPERIMENT STATION
UNIVERSITY OF ILLINOIS
URBANA, ILLINOIS

INTRODUCTION

This report presents an application of a circularly deflecting system to an analysis of an H.F. modulated electron beam with respect to its density and velocity distribution during one cycle at any given point on the beam.

The deflecting system, denoted as "phase writer" and reported elsewhere*, was designed to serve the purpose of circularly deflecting an H.F.-modulated electron beam with the same frequency as the beam is modulated, in order to obtain a conversion of each phase element somewhere on the beam into a separable geometrical deflection angle element. Thus, "phase writer" was considered an appropriate notation.

In Technical Report 5 2 "Chromatic and Space Charge Aberrations in Circularly Deflected Electron Beams" it was pointed out that any deflecting system of finite extensions will show a certain velocity sensitivity, i.e., the deflection angle will depend upon the velocity of the passing electrons. In the report mentioned above, this effect was treated in the sense of an aberration. However, a controlled aberration can be used as an indicator just as chromatic aberrations in a prism are essential for spectroscopy.

In this report it will be shown that the chromatic aberrations of the deflecting system in question can be utilized so that this system may serve not only as a phase writer system, but also as a velocity spectrograph. A system for experimental verification of these considerations was conveniently at hand and a series of experiments was carried out in which the bunching action in the drift region of a velocity modulated electron beam was made accessible to direct observation. These results were recorded in a set of photographs. Since a calibrated modulator provided the ac component of the velocity of the electrons in the beam, a comparison with a first order bunching theory could be made. The agreement of the observation with the theory is excellent as long as the effects have their cause in the action along the long drift space.

In the vicinity of "bunches", however, space charge effects begin to play a somewhat distorting role. The occurance of such phenomena is directly observable on the screen and can be carefully studied later on the photographic plate.

Since these experiments seem to represent a successful advance in the field of H.F. modulated beam analysis, it was decided to present this study in this Report.

---

*Contract N6-ori-71 Task XIX, Progress Reports 9 to 14; Technical Report No. 5-2.

TABLE OF CONTENTS

PART I
VELOCITY SENSITIVITY OF THE DEFLECTOR

H M Von Foerster

1. THE SYSTEM

A brief recapitulation of the essential features of the deflecting system may be appropriate. The principle of the deflecting mechanism consists of two pairs of shorted Lecher wires, placed perpendicular to each other and excited in such a manner that the maxima of the standing waves on both wire pairs fall on the cross point of the pairs. The electron beam is shot through the little square-shaped window which is formed by the edges of the wires. (See Fig. 1.)
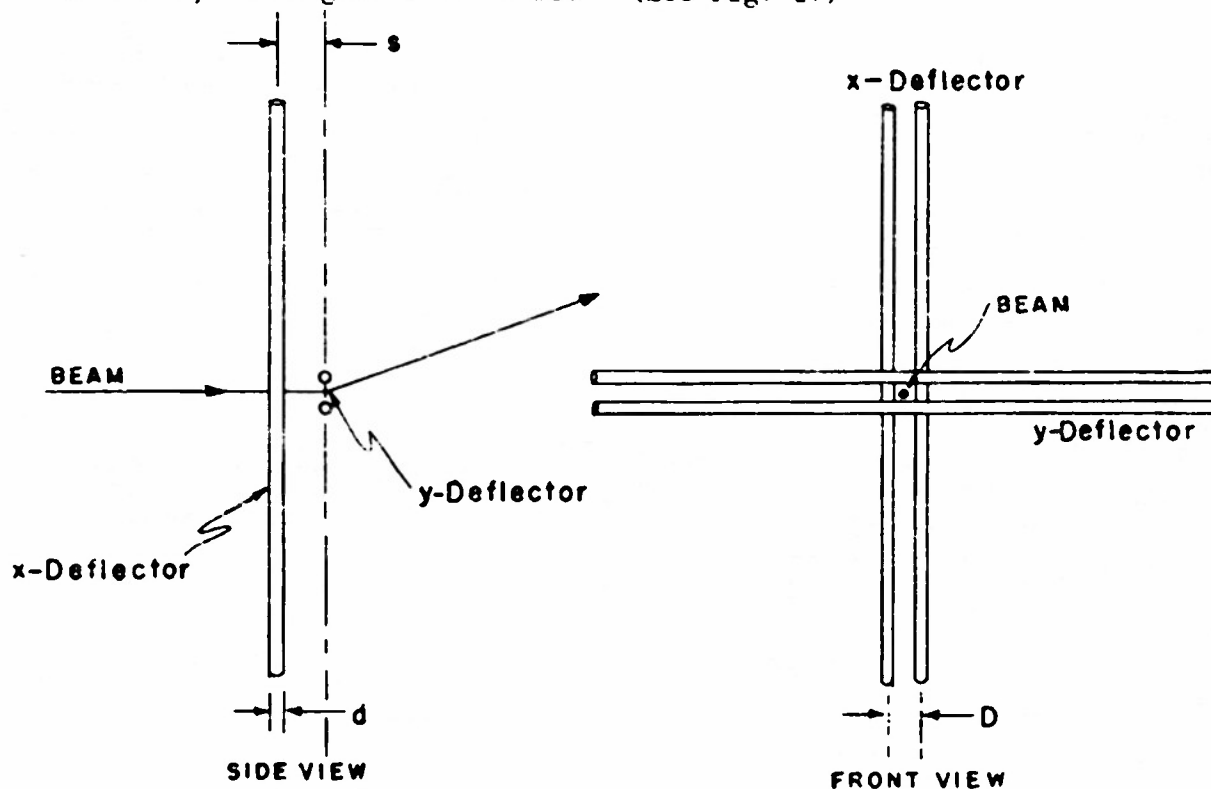
FIGURE 1   DEFLECTOR SYSTEM, SCHEMATICALLY

As has been shown in preceding reports, each wire pair will cause an electron beam with the voltage U to deflect R centimeters on a screen according to the formula

$$R = L \cdot A \cdot \sqrt{P_D} \; \frac{1}{U} \; e^{-2\sqrt{U_m/U}} \tag{1}$$

where

    L   is the distance from the wire pair to the screen in centimeters

    P_D is the power in watts fed into the deflector

    U   is the beam voltage in volts.

The symbols A and U_m represent constants defined by the geometry of the system. A, of minor importance in this context, can be approximated as

$$A = \frac{4\lambda}{D + d}$$

whereas

$$\sqrt{U_m} = \frac{\pi}{4} 10^3 \frac{D}{\lambda} \sqrt{1 + \frac{2d}{D}} \tag{2}$$

where

D is the spacing of the two wires

d is the diameter of one wire

λ is the free space wave length of the applied signal

It will be shown later that U_m represents the beam voltage which produces the maximum deflection for a given system. Operating at frequencies of about 3000 mcps U_m turns out to be of the order of hundreds of volts.

To demonstrate how the deflection R is related to the applied beam voltage, U, the function R = R(U) is plotted in Fig. 2. Both coordinates are normalized with respect to their maxima R_m and U_m. The maximum deflection R_m is readily obtained by inserting U_m for U in Eq. (1). One gets

$$R_m = \frac{AL \sqrt{P_D}}{U_m e^2} \tag{3}$$

If the two systems are simultaneously and equally strongly excited and oscillate with a phase difference φ_1, then an electron, passing the first system will accordingly be deflected in the x direction. After traveling the transit angle ϕ, the electron will be influenced by the second system which imposes on it deflections in the y direction. Taking the phase state φ of the x deflector as a reference time for all events along the beam, the locus of all electrons impinging on the screen after they have passed the two deflectors is thus:

$$x = R \cos \varphi \tag{4}$$

$$y = R \sin (\varphi - \varphi_1 + \phi) \tag{5}$$

R is the deflection in either direction and can be directly obtained from Eq. (1). Since φ_1 is the phase difference with which the two wire pairs are driven, φ_1 can be adjusted from outside by stretching the line feeding the y deflector. Choosing φ_1 so that

$$\varphi_1 = \phi \tag{6}$$

Eqs. (2) and (3) reduce to

$$x = R \cos \varphi$$
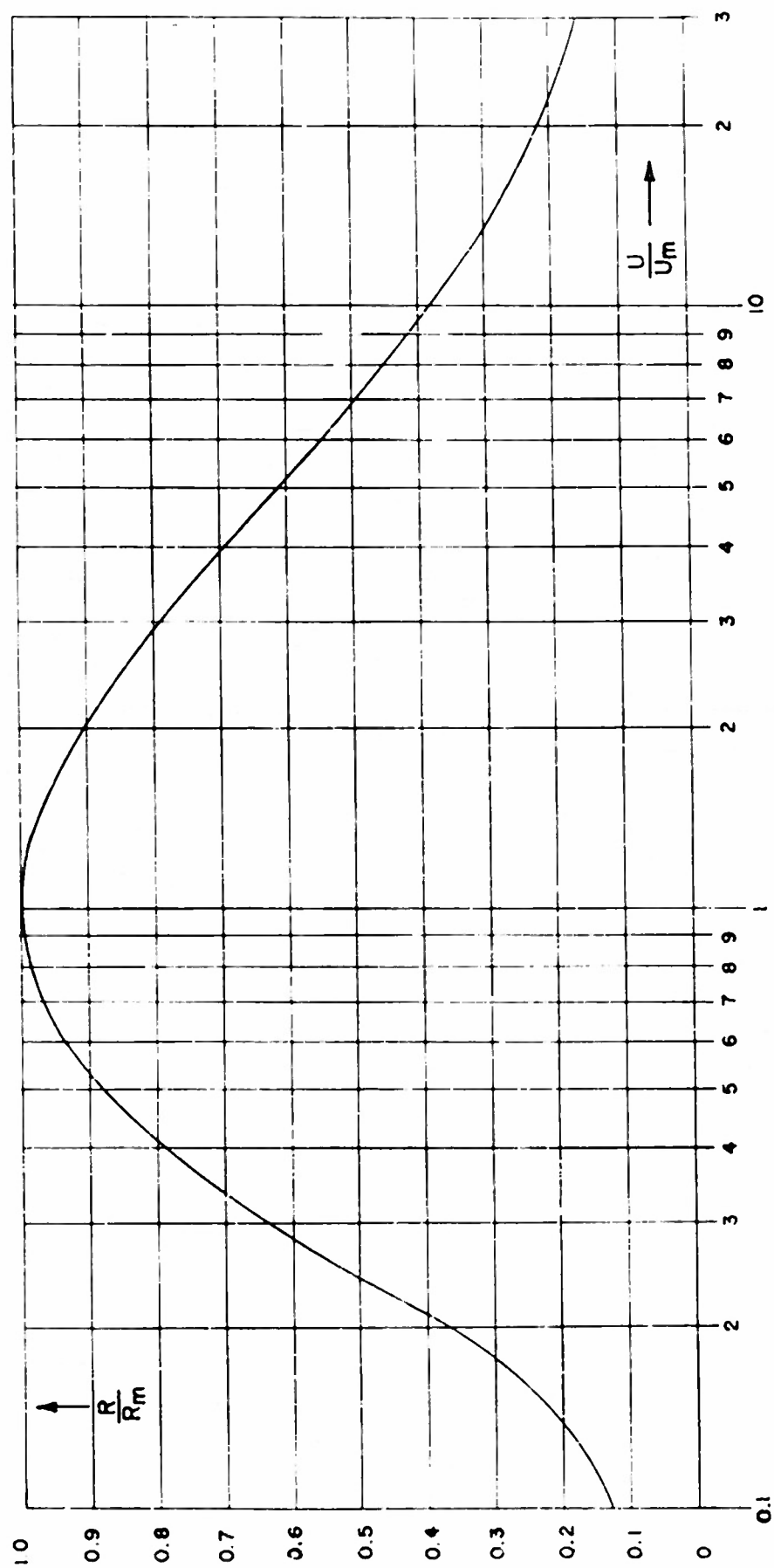$$y = R \sin \varphi \tag{7}$$

FIGURE 2   DEFLECTION AS A FUNCTION OF BEAM VOLTAGE
FOR A SINGLE DEFLECTION WIRE PAIR

and the display of the electrons impinging on the screen is a perfect
circle. The transit time φ of electrons between the two deflectors is,
of course, dependent on the velocity of the electrons, and can be
expressed as

$$\varphi = \frac{\sqrt{U_s}}{\sqrt{U}} \tag{8}$$

where U_s is a constant for a given system, depending on the distance s
between the wire pairs and the wave length λ in the following way:

$$\sqrt{U_s} = \pi \cdot 10^5 \frac{s}{\lambda} \tag{9}$$

U_s represents the beam voltage, which makes the drift space 1 radians
long.

Let us now consider that φ_1 has been adjusted so that for a par-
ticular beam voltage U_o the "circle condition" (Eq. 6) has been ful-
filled:

$$\varphi_1 = \phi_0 = \frac{\sqrt{U_s}}{\sqrt{U_o}}$$

Then, as was shown in Technical Report 5 2 page 37 electrons having a
different energy, say U_1 will display themselves along an ellipse, the
major axis of which will be declined 45 degrees against the xy deflec-
tors and will fall either into the (+ +) (− −) quadrants or (+ −) (− +)
quadrants, depending on whether U_1 is higher or lower than U_o. (See
Fig. 3.)
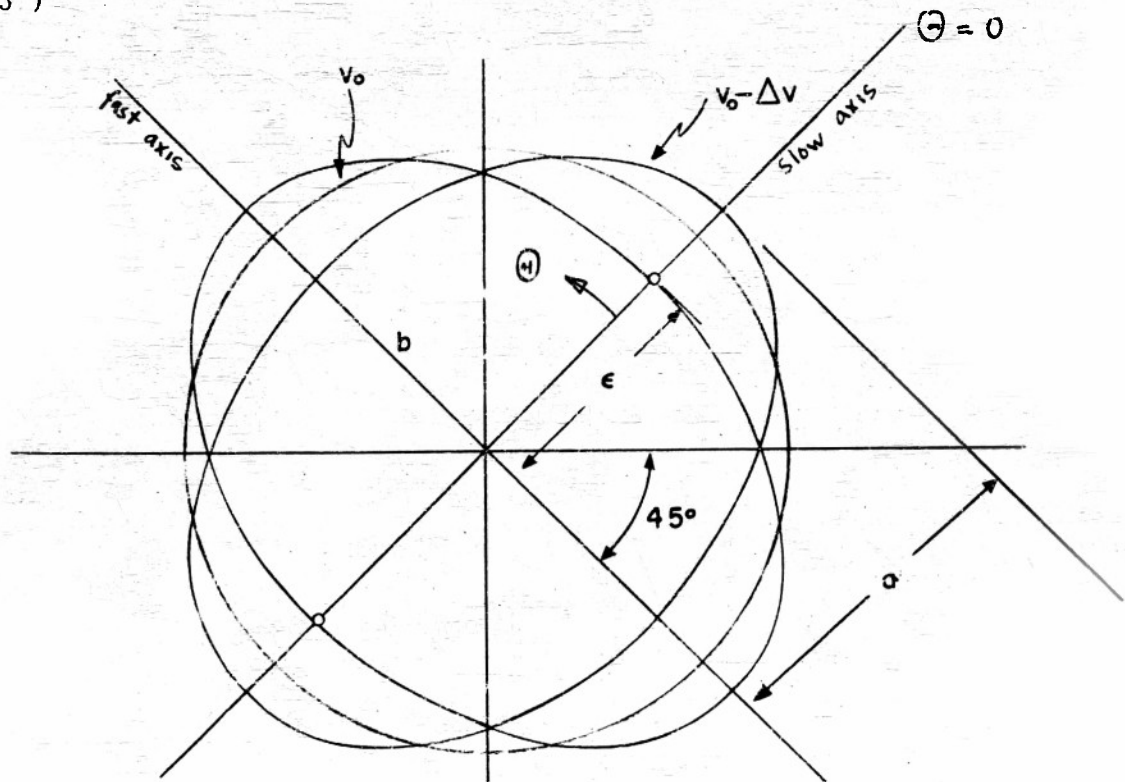
FIGURE 3   THE LOCUS OF ALL POINTS DEFINED BY ARRIVING ELECTRONS
HAVING A VELOCITY V = $V_0 \pm \Delta v$

The magnitude of the major and minor axes can be computed to

$$a = R \sqrt{1 + \sin \delta}$$

$$b = R \sqrt{1 - \sin \delta} \qquad (10)$$

where δ is the increment of transit angle which was gained or lost due to faster or slower electrons passing the two wire pairs

$$\delta = \phi_1 - \phi_0 = \frac{\sqrt{U_s}}{\sqrt{U_1}} - \frac{\sqrt{U_s}}{\sqrt{U_0}}$$

for

$$U_0 > U_1 \qquad (11)$$

$$\delta = \phi_0 - \phi_1 = \frac{\sqrt{U_s}}{\sqrt{U_0}} - \frac{\sqrt{U_s}}{\sqrt{U_1}}$$

for

$$U_1 > U_0 .$$

If the difference in the energy of electrons in the beam is small

$$|U_1 - U_0| = \Delta U$$

δ can be approximated to

$$\delta = \frac{1}{2} \phi_c \frac{\Delta U}{U_0} . \qquad (12)$$

2   VELOCITY SENSITIVITY

In the preceding section it was shown that the velocity of the electrons passing through the system of the two perpendicular crossed wires enters the description of the deflection in a twofold way:

a   according to Eq (4) which describes the deflection R as a function of the velocity in a single deflector

b   according to Eqs (10) and (11) which describe the deflection behaviour of the combined action of the two crossed deflectors.

The over all velocity sensitivity of the two combined effects can be described as

$$dR = \left(\frac{\partial R}{\partial U}\right)_I dU + \left(\frac{\partial R}{\partial U}\right)_{II} dU \tag{13}$$

if the indices I and II refer to the single and the double pair action respectively

2.1   Velocity Sensitivity of a Single Pair

The expression $\left(\frac{\partial R}{\partial U}\right)_I$ can be found immediately by differentiating Eq (4) with respect to U   One obtains

$$\left(\frac{\partial R}{\partial U}\right)_I = \frac{R_o}{U_o}\left(\sqrt{\frac{U_m}{U_o}} - 1\right). \tag{14}$$

The significance of U_m now becomes evident   For $U_o = U_m$, the right hand side of Eq (14) vanishes which can be interpreted in two equiv-alent statements

a   At that point of operation the deflection of a single wire pair is independent of the electron velocity

b   Vanishing of the first differential quotient indicates opera-tion at the maximum of deflection

2 2   Velocity Sensitivity of the Double Pair

Defining the resulting ellipse in coordinates ξ, η which are 45° declined to the two deflectors and immediately replacing ξ by r cos θ and η by r sin θ, where r is the distance from the origin to any point of the ellipse $\theta°$ away from one of the new axes using Eq (10) for a and b one obtains

$$\frac{r^2 \cos^2\theta}{1+\delta} + \frac{r^2 \sin^2\theta}{1-\delta} = R^2. \tag{15}$$

After simple trigonometric transformations the change of the radius $\Delta R = r - R$ as a function of δ and the azimuth θ is obtained:

$$\Delta R = R_o\left(\frac{\cos\delta}{\sqrt{1 + \sin\delta\cos(2\theta)}} - 1\right). \tag{16}$$

Assuming δ to be small, thus using Eq. (12), approximating

$$\sin \delta \approx \delta$$

$$\cos \delta \approx 1$$

and expanding the square root, Eq. (16) reduces to

$$\left(\frac{\partial R}{\partial U}\right)_{II} = -\frac{R_o}{U_o} \cdot \frac{1}{4} \frac{\sqrt{U_s}}{\sqrt{U_o}} \cos (2\theta) \tag{17}$$

for small velocity changes.

It may be noted that the velocity sensitivity of the double system is a function of the azimuth θ and assumes extrema along the axes of the ellipse, where $\theta = 0, \frac{\pi}{2}, \pi, \frac{3\pi}{2} \cdots$.

2 3 Velocity Sensitivity of the Whole System

To establish the velocity sensitivity of the whole system as a function of the different parameters involved it is necessary only to insert the results of the two preceding paragraphs, i e Eqs. (14) and (17) into Eq. (13). This yields

$$\frac{dR}{R_o} = -\frac{dU}{U_o} \left(1 + \frac{\frac{1}{4} \sqrt{U_s} \cos (2\theta) \cdot \sqrt{U_m}}{\sqrt{U_o}}\right) \tag{18}$$

Defining the relative velocity sensitivity σ by

$$\sigma = -\left(\frac{dR}{dU}\right) \cdot \frac{U_o}{R_o} \tag{19}$$

It may be seen from Eq. (18) that σ depends on the two apparatus constants $\sqrt{U_s}$ and $\sqrt{U_m}$ and on the voltage of the beam U_o. Furthermore σ will have different values along the periphery of the original circle, depending on the azimuthal angle θ. Along the "slow axis" ($\theta = 0$)* the relative velocity sensitivity σ becomes

$$\sigma_{Slow} = 1 + \frac{\sqrt{U_\Delta}}{\sqrt{U_o}} \tag{20}$$

Along the "fast axis" ($\theta = 90°$) the result is

$$\sigma_{Fast} = 1 - \frac{\sqrt{U_s}}{\sqrt{U_o}} \tag{21}$$

* See Fig. 3

8

where

$$\sqrt{U_A} = \sqrt{U_s/16} - \sqrt{U_m}$$

$$\sqrt{U_?} = \sqrt{U_s/16} + \sqrt{U_m}$$

(22)

From Eqs (20) and (21) it is obvious that the highest velocity sensitivity is expected along the "slow axis" Conversely, a smaller velocity sensitivity is expected along the "fast axis" This is understandable because in the "slow case" the two separate causes, (single pair double pair) add up whereas in the "fast case" they compensate each other

In constructing a system the relative velocity sensitivity desired must be considered The selection U_m is somewhat inflexible since it has a limited range However an almost unlimited range is available with the selection of $\sqrt{U_s}$ (i e a particular distance between the two wire pairs) in order to meet the sensitivity requirements

In Fig 4 the values of σ_{Fast} and σ_{Slow} are given for different $\sqrt{U_s}$ as a function of the beam voltage U_0 whereby U_m was assumed to be 312 volts

In Fig 5 σ along the periphery of the circle is drawn for two different beam voltages ($U_0 = 1000$ volts) ($U_0 = 3000$ volts) and for fixed values of the two constants $\sqrt{U_s}$ and $\sqrt{U_m}$ They were selected to be the values of the system with which the experimental studies were carried out

$$(\sqrt{U_s} = 185\ 2\ \text{volts}^{1/2} \qquad \sqrt{U_m} = 17\ 6\ \text{volts}^{1/2})$$
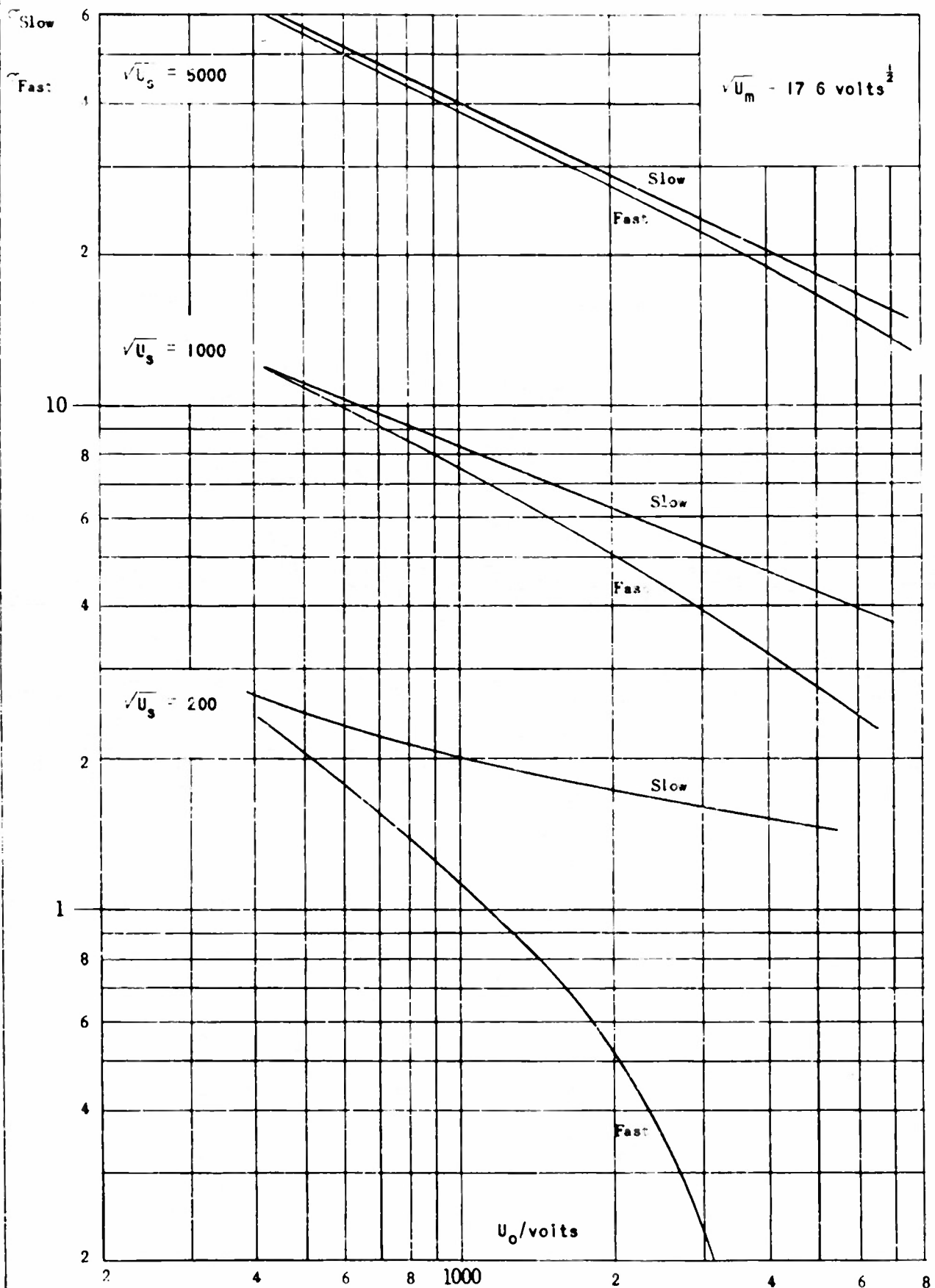
FIGURE 4   RELATIVE VELOCITY SENSITIVITY ALONG THE "FAST" AND "SLOW" AXES AS A FUNCTION OF THE BEAM VOLTAGE U_0 FOR DIFFERENT PARAMETERS $\sqrt{U_s}$
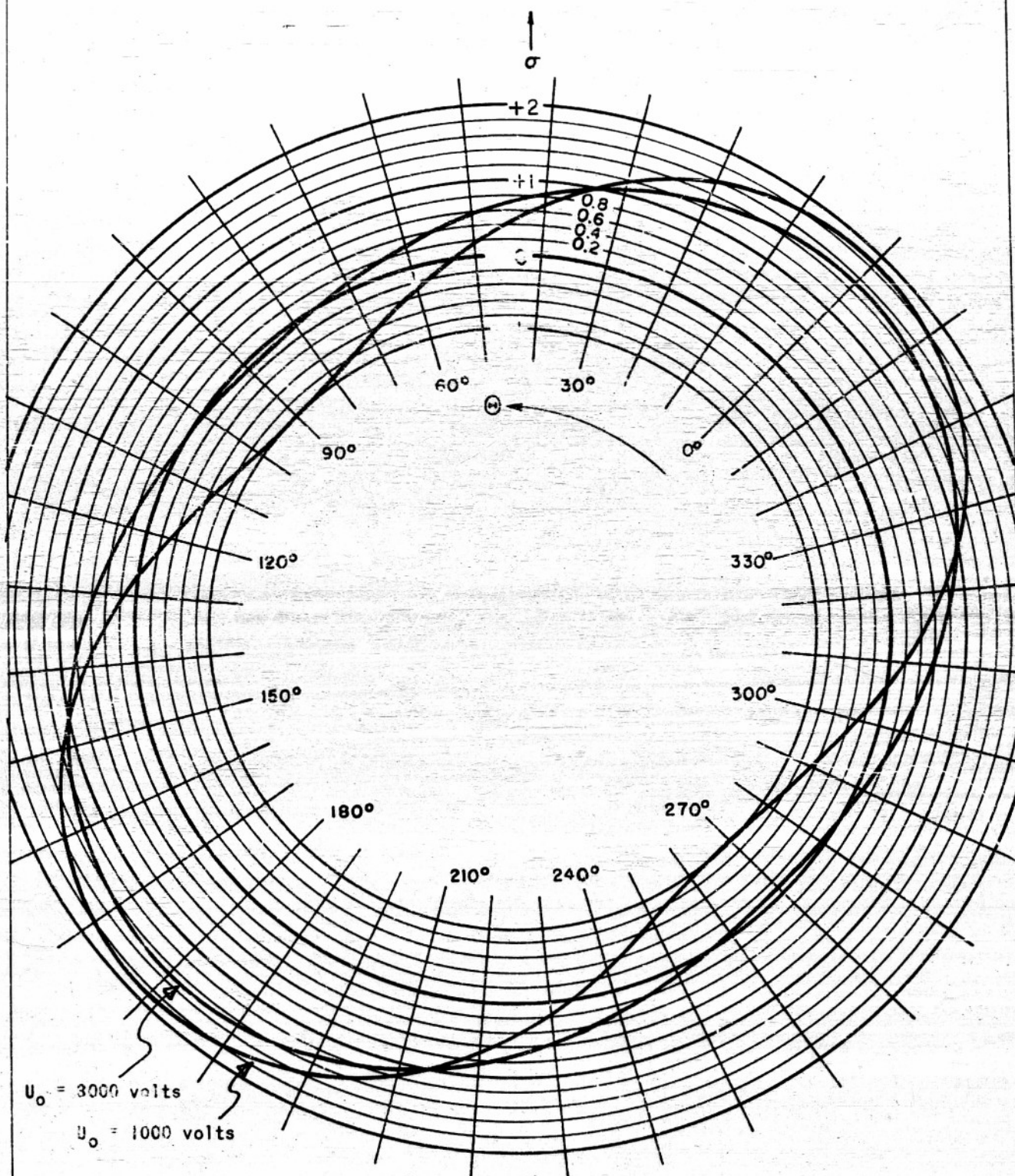
FIGURE 5   RELATIVE VELOCITY SENSITIVITY AS A FUNCTION
OF THE AZIMUTHAL ANGLE θ FOR TWO BEAM VOLTAGES AND FIXED VALUES
$\sqrt{U_S}$ = 185 2 VOLTS$^{1/2}$ AND $\sqrt{U_a}$ = 17 8 VOLTS$^{1/2}$

3. EXPERIMENTAL DETERMINATION OF $\sqrt{U_m}$ AND $\sqrt{U_s}$

In the preceding section it was shown that the two constants

$$\sqrt{U_m} = \frac{\pi}{4}\ 10^3\ \frac{D}{\lambda}\ \sqrt{1 + \frac{2d}{D}} \tag{2}$$

and

$$\sqrt{U_s} = \pi \cdot 10^3\ \frac{s}{\lambda} \tag{9}$$

play a decisive role in the response of the double Lecher-system to velocity changes. To use the system as a calibrated velocity-analyzer it is therefore necessary to check the accuracy with which the two constants can be determined by studying the performance of the system mentioned previously. Comparing these results with a simple determination of $\sqrt{U_m}$ and $\sqrt{U_s}$ according to Eqs. (2) and (9) by mechanical measurement one has a measure for the accuracy of the operation of that system.

A system which was constructed for a particular study reported elsewhere * was available in this laboratory and had geometrical dimensions which seemed feasible for such an experiment. A 1:10 enlargement of this system is given in Fig. 6 and a photographic reproduction in Fig. 7.

The dimensions in question are

$$d = 0.155\ cm$$
$$D = 0.129\ cm$$
$$s = 0.629\ cm$$

and the free space wave length by which all of the following experiments were carried out is

$$\lambda = 10.51\ cm$$

These values give the following theoretical data for $\sqrt{U_m}$ and $\sqrt{U_s}$

$$\sqrt{U_m} = 17.6$$
$$\sqrt{U_s} = 185.3. \tag{23}$$

The following two paragraphs will discuss the possibility of experimentally determining the numerical value of these two constants

3.1 Determination of U_m

The value U_m controls the behaviour of one single wire pair and can be determined by driving one pair at a time. The simplest way to find the numerical value of U_m would be to vary the beam voltage U until a maximum deflection is seen on the screen. This method would give only very approximate results since the maximum of the $R(U)$ - function is

*See Final Report on Millimeter Wave Research. Air Force Cambridge Research Center Contract No AF 19(122)-5 Chapter I
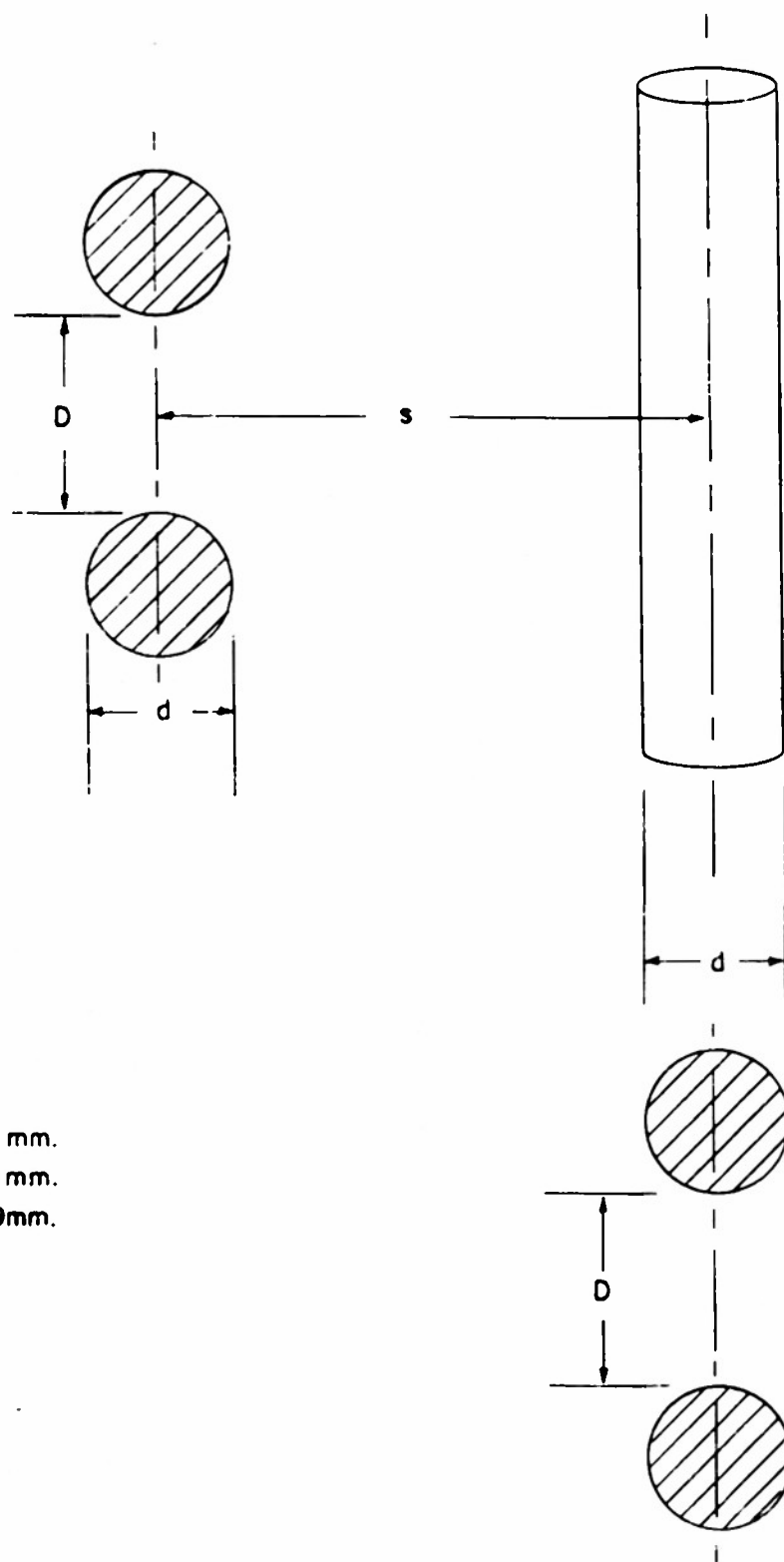
d= 1.55 mm.
D= 1.29 mm.
s = 6.29mm.

FIGURE 6   DETAIL DRAWING OF THE COMPLETE DEFLECTOR SYSTEM
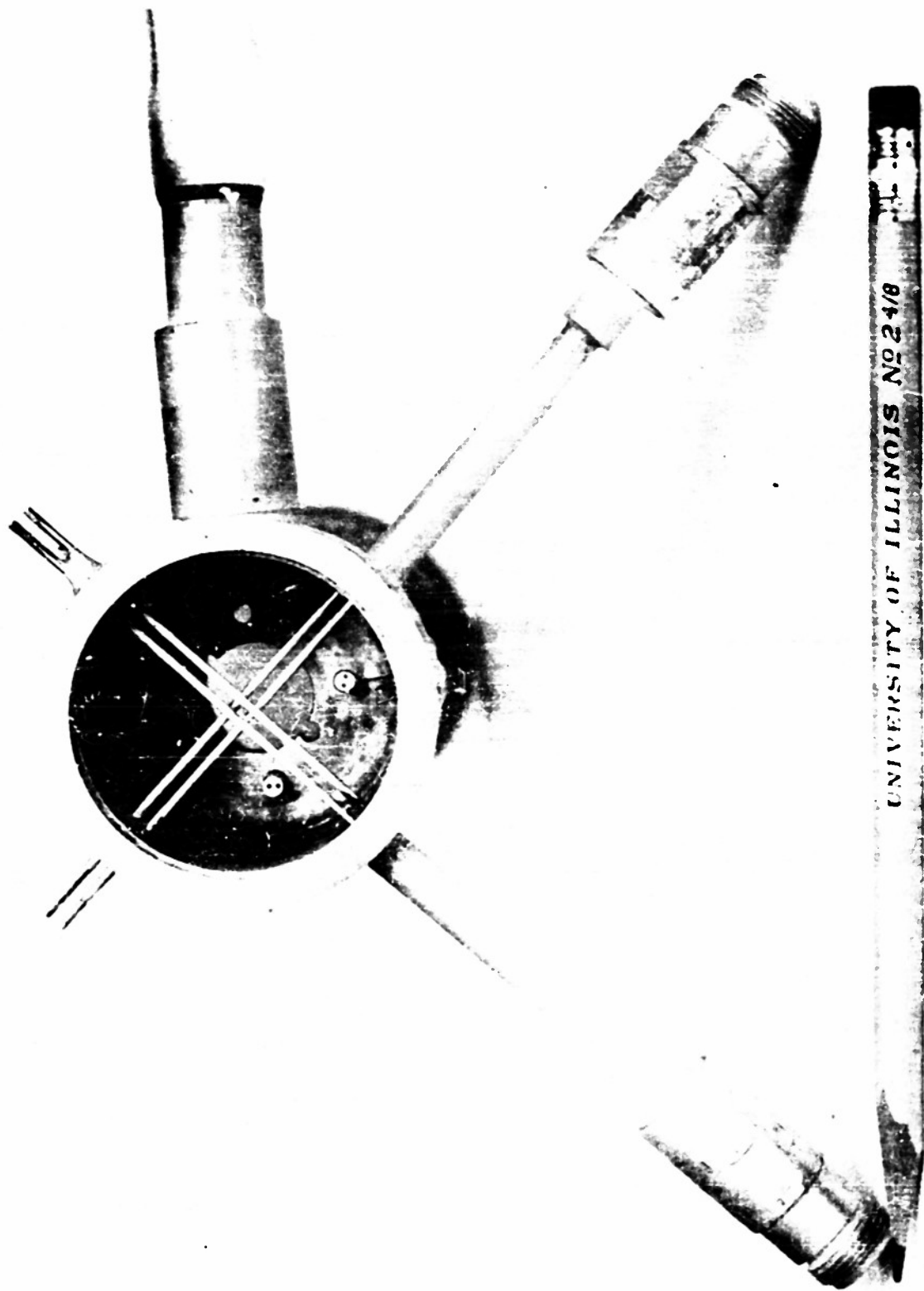
SCALE   10 1

-13-

UNIVERSITY OF ILLINOIS No 248

FIGURE 7   THE DEFLECTOR SYSTEM

very flat (see Fig 2) Furthermore at about 300 volt beam voltage
the electron beam would leave an almost unobservable trace on the
screen   Thus another line of attack had to be designed   The method can
be outlined as follows

Take the logarithm of the square root of Eq   (1)

$$\tfrac{1}{2} \ln R = \tfrac{1}{2} \ln (AL \sqrt{P_D}) + \ln \frac{1}{\sqrt{U}} \qquad \frac{\sqrt{U_m}}{\sqrt{U}} \qquad (24)$$

and differentiate with respect to $1/\sqrt{U}$

$$\frac{\tfrac{1}{2} d \ln R}{d \left(\frac{1}{\sqrt{U}}\right)} = \sqrt{U} - \sqrt{U_m} . \qquad (25)$$

Plotting $\tfrac{1}{2} d(\ln R) / d (1/\sqrt{U})$ against $\sqrt{U}$ one should obtain a straight
line with the slope 1 cutting the abscissa exactly at the desired
quantity $\sqrt{U_m}$ This method has the advantage of being very accurate in
the vicinity of U_m Furthermore the final determination of $\sqrt{U_m}$ through
Eq (25) does not require the knowledge of the quantity $AL \sqrt{P_D}$

The experimental procedure was as follows
One wire pair at a time was excited with a constant power   The
deflection R was photographically registered on a screen for different
beam voltages   A set of such photographs is reproduced in Fig 8   The
deflection R can now be taken from any enlargement since the absolute
values of R do not appear in Eq (25)

Plotting log R against $1/\sqrt{U}$ a representation of Eq (24) is ob-
tained   Graphical differentiation of these curves gives the ordinates
of Eq (25) Finally Fig 9 gives a representation of Eq (25) for the
measured values in the vicinity of U_m The unit of U was taken to be
100 volts and the factor 2 3 in the ordinate accounts for plotting log R
on a $\log_{10}$ paper   The measured values were evaluated according to Gauss
method of least squares and the resulting line is plotted heavily on
Fig 9   It crosses the abscissa at $\sqrt{U_m/100} = 1\ 84$, thus

$$(U_m)_{Exp} = 339 \pm 23 \text{ volts}$$

From Eqs (2) and (23) we obtain

$$(U_m)_{Th} = 317 \text{ volts}$$

the expected value of U_m computed from the geometrical data   The
deviation of 7% lies well within the accuracy of the measurement   But
more important than a good agreement of the quantity U_m is the consi-
deration that the observed values follow a straight line with the slope
1 so well   This is further confirmation that the considerations from
which Eq (1) is derived seem to be sound

	U_o/volts
	2200
	1800
	1500
	1200
	1000
	800
	600
	500
	400
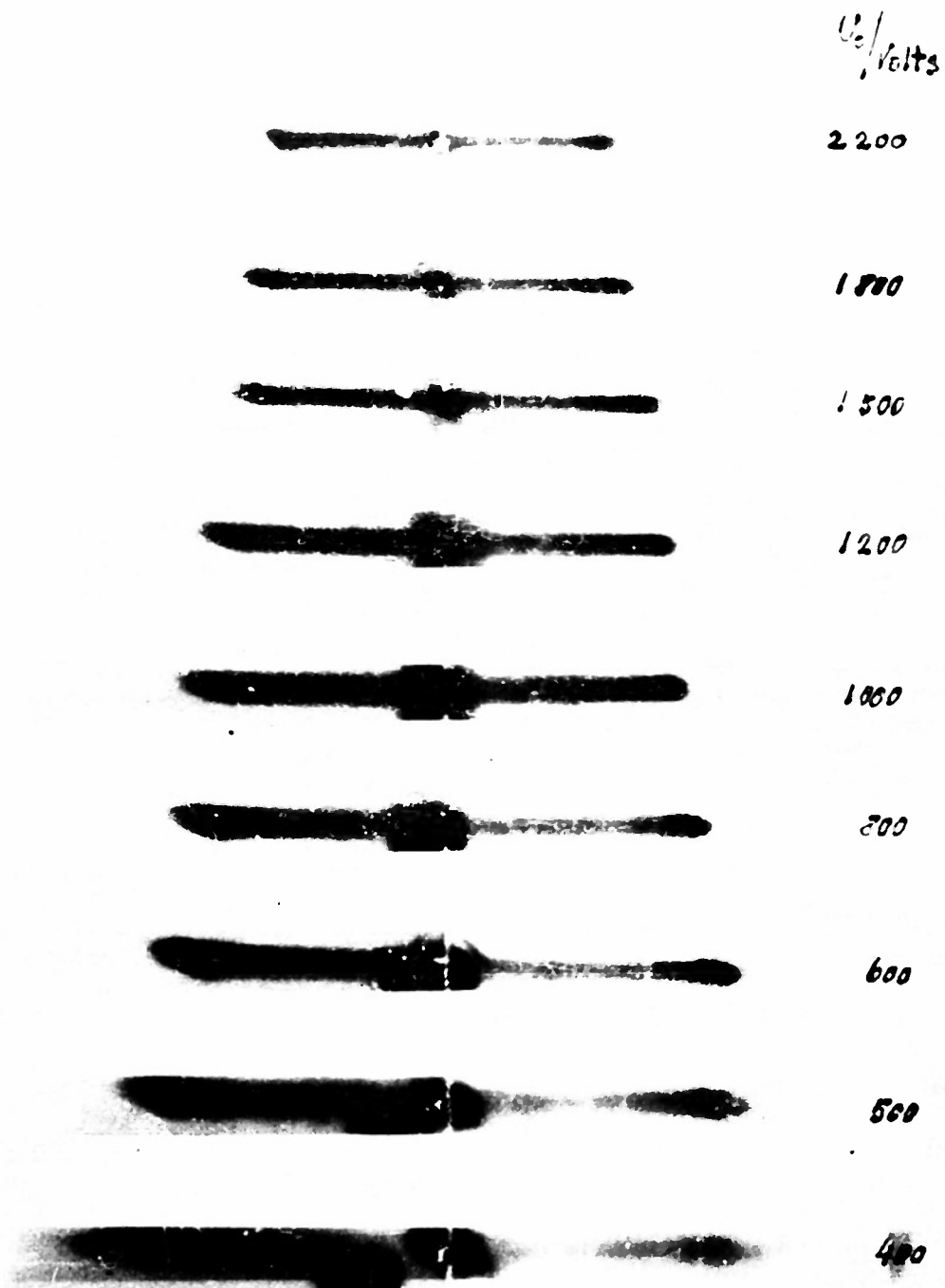
FIGURE 8   DEFLECTION OF THE Y-DEFLECTOR FOR DIFFERENT BEAM VOLTAGES U_o

FIGURE 9   GRAPHICAL DETERMINATION OF $\sqrt{U_{min}}$

$$\frac{2.3}{2} \cdot \frac{d \log_{10} R}{d \frac{1}{\sqrt{U/100}}}$$

△ Y-Deflector
○ X-Deflector

$\sqrt{U/100} \longrightarrow$
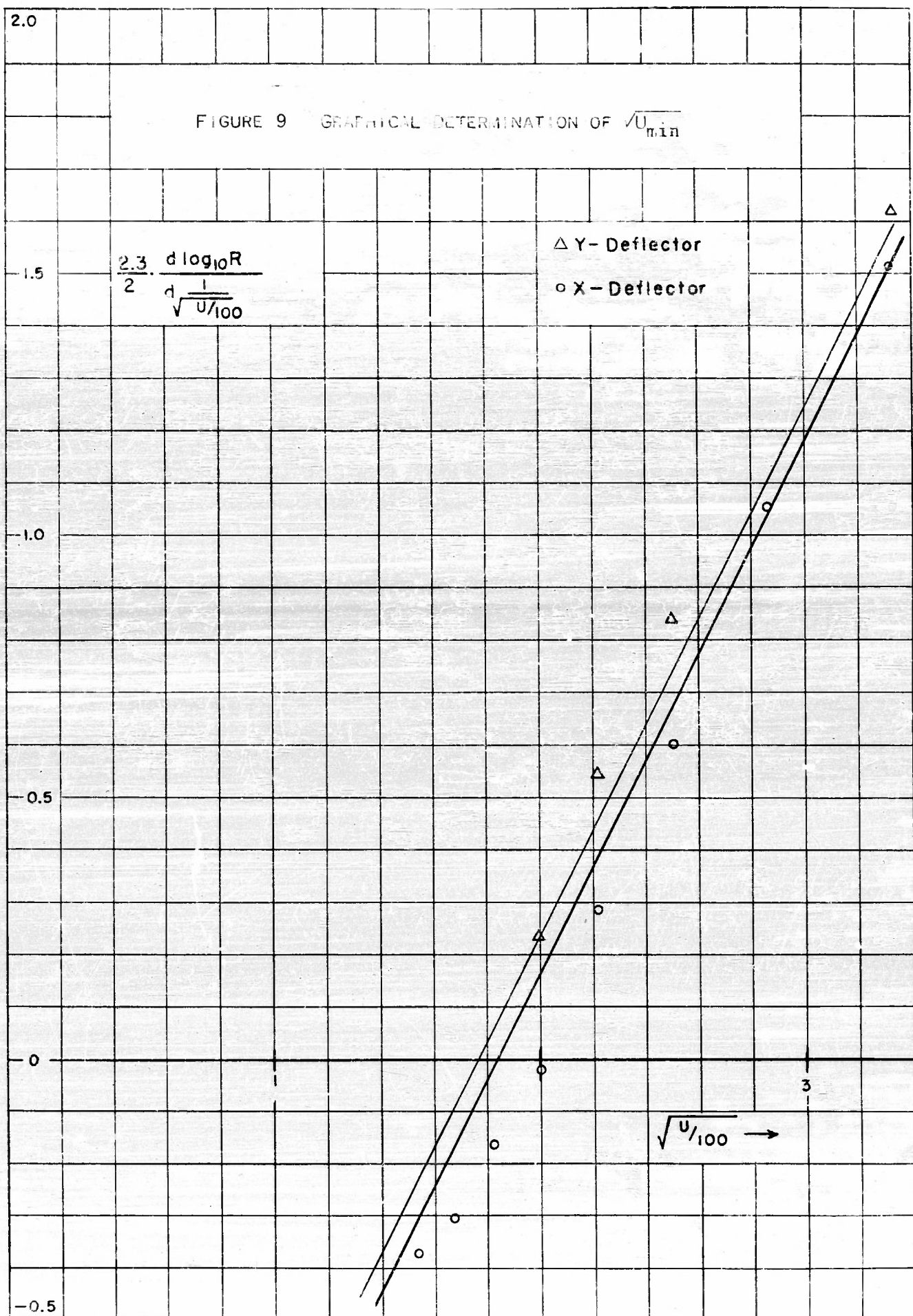
3.2 Determination of $\sqrt{U_s}$

The value $\sqrt{U_s}$ controls the transit angle of electrons passing from one wire pair to the other. As was shown before $\sqrt{U_s}$ is a decisive element in the equation defining the velocity sensitivity of the whole system. (See Eq. (18) and Fig. 4) An accurate determination of $\sqrt{U_s}$ from an experimental point of view would therefore be desirable. The two equations

$$\delta = \frac{\sqrt{U_s}}{\sqrt{U_o}} - \frac{\sqrt{U_s}}{\sqrt{U_o}} \tag{11}$$

$$a = R\sqrt{1 + \sin \delta}$$
$$b = R\sqrt{1 - \sin \delta} \tag{10}$$

suggest the possibility of determining $\sqrt{U_s}$ by observable data. With Eq. (11) one obtains

$$\sqrt{U_s} = \left| \delta \frac{\sqrt{U_1 U_o}}{\sqrt{U_o} - \sqrt{U_1}} \right| \tag{26}$$

Since δ can be determined by measuring the major and minor axes of the obtained ellipses through Eq. (10) all quantities are measurable to define $\sqrt{U_s}$.

Unfortunately this method would require knowledge of R at different voltages and thus U_m would enter into the final result. To avoid that a very elegant method could be suggested.

In Eq. (10) let δ become $\pm \frac{\pi}{2}$. Then for $\delta = +\frac{\pi}{2}$ b degenerates to 0 for $\delta = -\frac{\pi}{2}$ a degenerates to 0. In other words the ellipses in the two cases would degenerate to straight lines which are perpendicular to each other. Calling the two voltages of the beam U_1 and U_2 at which these lines occur $\sqrt{U_s}$ is given to

$$\sqrt{U_s} = \pi \frac{\sqrt{U_1 U_2}}{\sqrt{U_1} - \sqrt{U_2}} \tag{27}$$

since the total phase change δ in the system was π.

This method has the advantage of being completely independent of the change in R since it is only necessary to observe when the ellipses degenerate to lines. This point is extremely sensitive in its adjustment as can be seen by differentiating b in Eq. (10) with respect to δ

$$\frac{db}{d\delta} = \frac{R \cos \delta}{2\sqrt{1 - \sin \delta}} \tag{28}$$

-18-

for $\delta \to \frac{\pi}{2}$ (the 'line condition') $db/d\delta$ becomes infinity. Experimentally this expresses itself in a high instability of the line. A slight change in voltage immediately flips the line into an ellipse with a well observable minor axis.

Unfortunately this extremely accurate technique could not be applied because the insulation of the system limited the application of high voltage to about 2600 volts and the required voltage change to produce a total phase change of π in the system was too high.

A similar but less accurate method was therefore applied namely to produce a phase shift of only $\pi/2$ which would cause a circle to degenerate into a line.

Collecting a set of voltage pairs (U, U_o) which transform a circle into a line or vice versa $\sqrt{U_s}$ is given by

$$\sqrt{U_s} = \frac{\pi}{2} \frac{\sqrt{U}.\sqrt{U_o}}{\sqrt{U} - \sqrt{U_o}} \tag{29}$$

A set of 20 pairs of U, U_o were collected and the mean value of $\sqrt{U_s}$ computed. The result is

$$(\sqrt{U_s})_{Exp} = 185.8 \pm 4.6 \text{ volts}^{½}$$

This value is in good agreement with the theoretical value computed according to Eq. (9) from the geometrical data

$$(\sqrt{U_s})_{Th} = 185.3$$

Figures 10 and 11 illustrate such a phase change of $\pi/2$ with two intermediate stages. Note also the high velocity sensitivity along the 'slow axis' and the small sensitivity along the 'fast axis" as pointed out before. For technical reasons it was easier to swing the beam clockwise instead of counter clockwise. That makes θ negative with respect to the orthodox definition and thus the axes are exchanged as shown in Figs. 10 and 11. Figure 10 especially markedly shows the almost complete compensation of the two different velocity responses of the single and double system along the fast axis.

3 3 Check of the Influence of Both $\sqrt{U_m}$ and $\sqrt{U_s}$

To check the influence of both constants $\sqrt{U_m}$ and $\sqrt{U_s}$ on the performance of the beam several elliptical cases were studied. One will be reported here. The beam voltage was chosen to be 2000 volts, a circle was adjusted and a picture taken. Then the beam voltage was changed to 1700 volts and to 2300 volts and a picture on the same negative was taken in each case. Now δ was computed according to the exact Eq. (11) in both cases using the theoretical value of $\sqrt{U_s} = 185.3$. According to Eq. (11)

'Fast' case

$$\delta_F^\circ = 57.3 \left[\frac{185.3}{\sqrt{2000}} - \frac{185.3}{\sqrt{2300}} \right] = 16°.$$

Slow Axis

Fast Axis

SUPERPOSITION OF FOUR MONOCHROMATIC ELECTRON
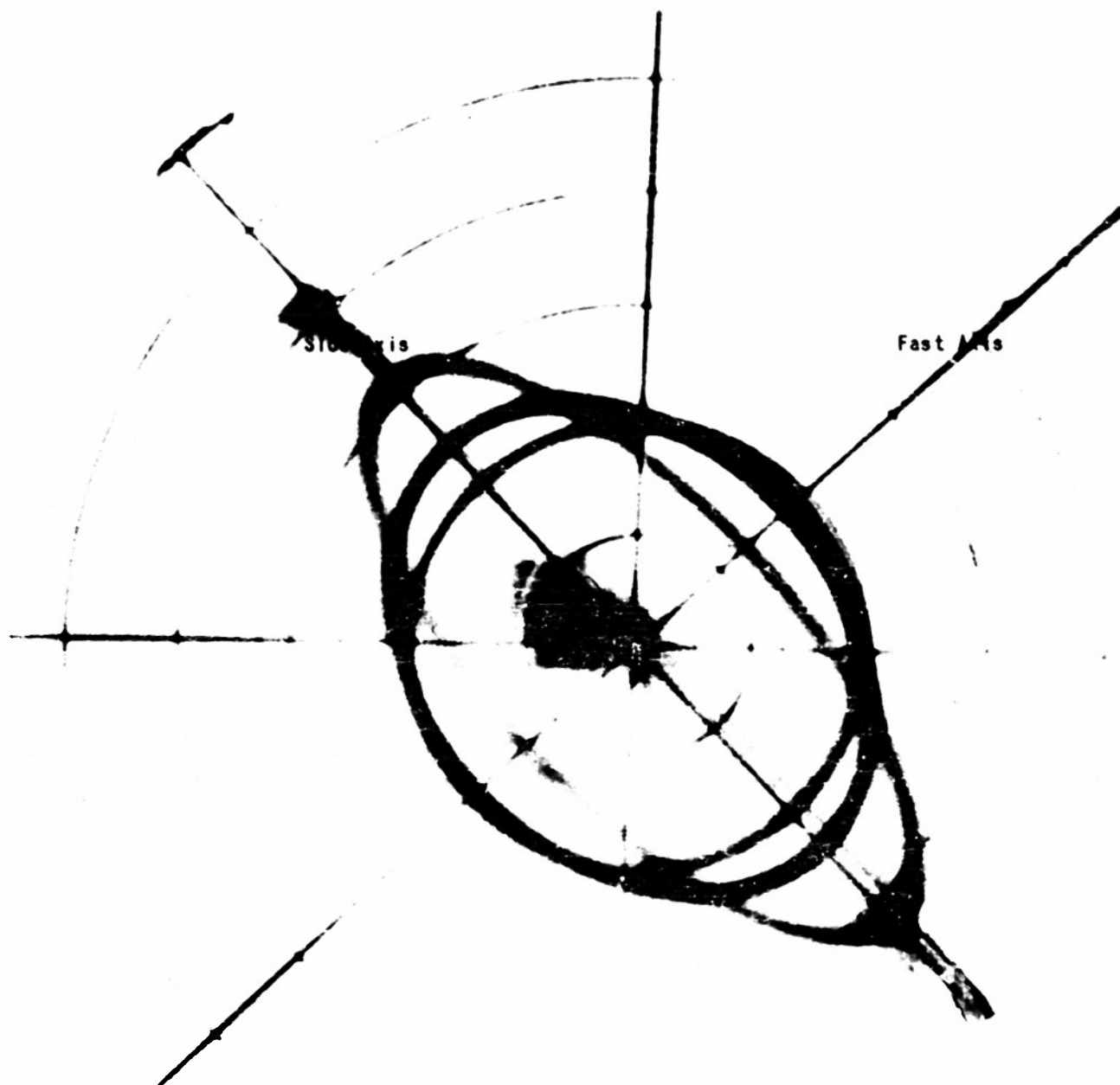BEAMS HAVING THE VELOCITIES
$U_0 = 1250$ VOLTS (CIRCLE)

U_1 1500 VOLTS

FIGURE 10 U_2 2000 VOLTS

$U_3 = 2400$ VOLTS (LINE)

TOTAL PHASE CHANGE IN THE SYSTEM $\pi/2$

Labels on figure: "Slow Axis", "Fast Axis"

SUPERPOSITION OF FOUR MONOCHROMATIC ELECTRON
BEAMS HAVING THE VELOCITIES

U_0 = 2550 VOLTS   (CIRCLE)

U_1 = 2250 VOLTS

FIGURE 11 U_2 = 1700 VOLTS

U_3 = 1230 VOLTS   (LINE)

TOTAL PHASE CHANGE IN THE SYSTEM $\pi/2$

"Slow" case

$$\delta_S^{\circ} = 57.3 \; \frac{185.3}{\sqrt{1700}} \; \frac{185.3}{.2000} = 20^{\circ}.$$

With these values of δ_S and δ_F the two quantities can be computed

$$\left(\frac{a}{b}\right)_{Fast} = \frac{R_F}{R_F} \frac{\sqrt{1 + \sin \delta_F}}{\sqrt{1 - \sin \delta}} = 1.34$$

$$\left(\frac{a}{b}\right)_{Slow} = \frac{R_S}{R_S} \frac{\sqrt{1 + \sin \delta_S}}{\sqrt{1 - \sin \delta_S}} = 1.43 .$$

Since R_S and R_F cancel in each case, the single-pair sensitivity does not enter here.

Measuring the developed and enlarged photograph the following values were obtained

$$\left(\frac{a}{b}\right)_{Fast} = 1.34 + 0.02$$

$$\left(\frac{a}{b}\right)_{Slow} = 1.46 \pm 0.02$$

in good agreement with the theoretical value.

The single-pair sensitivity enters if the dimensions in the fast and the slow case are compared. Computing R_F and R_S according to Eq. (14)

$$\frac{R_S}{R_F} = \frac{1 + \frac{\Delta U}{U_o} \; 1 \; \sqrt{\frac{U_m}{U_o}}}{1 \; \frac{\Delta U}{U_o} \; 1 - \sqrt{\frac{U_m}{U_o}}} . \tag{30}$$

With $\Delta U = 300$, $U_o = 2000$ and the theoretical value of $\sqrt{U_m} = 17.6$ then, theoretically

$$\left(\frac{R_S}{R_F}\right)_{Th} \quad 1.205$$

With this value and knowing δ_S and δ_F the two quantities can be computed

$$\left(\frac{a_S}{a_F}\right)_{Th} = \frac{h_s}{1} \frac{\sqrt{1 + \sin \delta_S}}{\sqrt{1 + \sin \delta_F}} = 1.231$$

and

$$\left(\frac{b_S}{b_F}\right)_{Th} = \frac{R_S}{R_F} \frac{\sqrt{1 - \sin \delta_S}}{\sqrt{1 - \sin \delta_F}} = 1.155 .$$
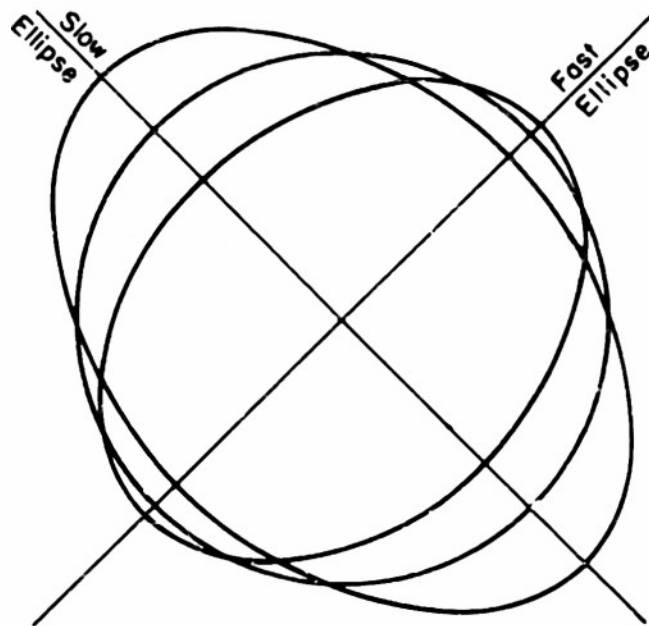
FIGURE 12a   THEORETICAL PICTURE OF THE SUPERPOSITION OF THREE
MONOCHROMATIC ELECTRON BEAMS HAVING THE VELOCITIES:

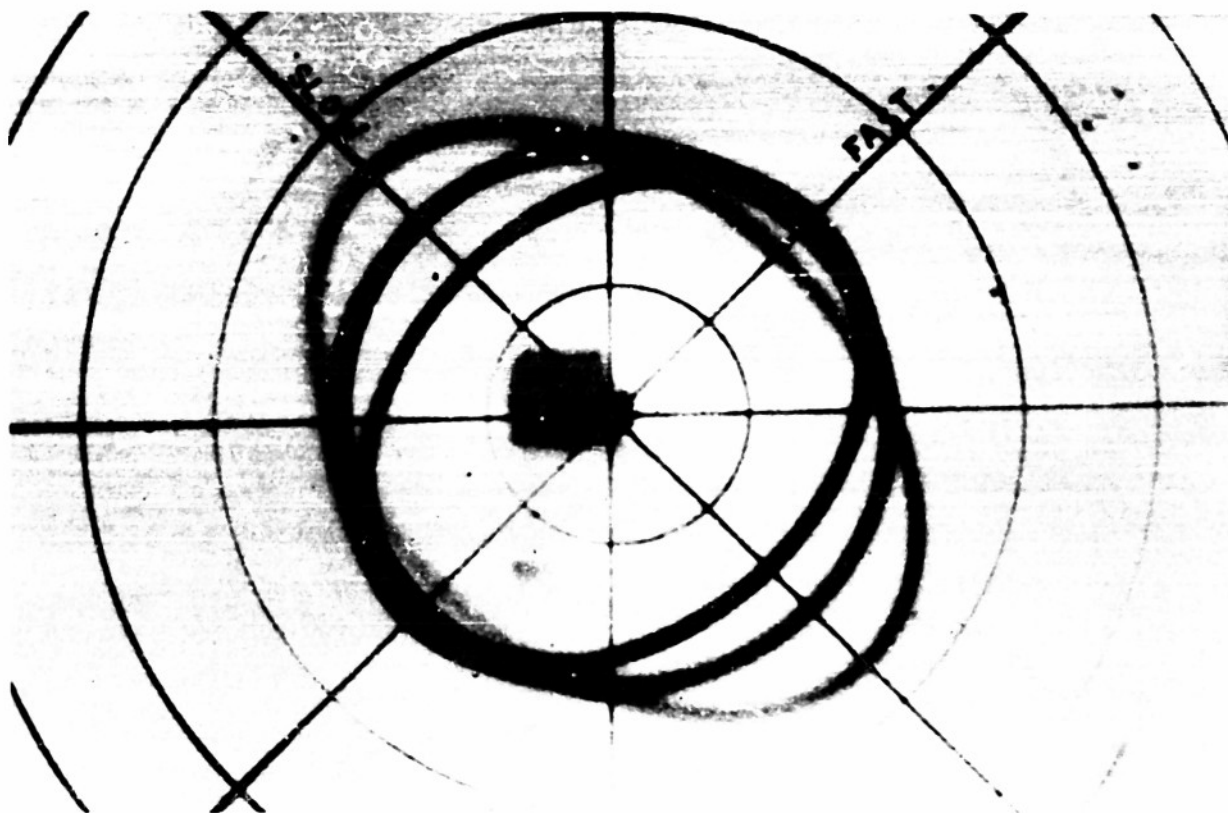U_1 = 1700 VOLTS; U_o = 2000 VOLTS (CIRCLE); U_2 = 2300 VOLTS

FIGURE 12b   OBSERVED PICTURE OF THE SUPERPOSITION OF THREE
MONOCHROMATIC ELECTRON BEAMS HAVING THE VELOCITIES:

U_1 = 1700 VOLTS; U_o = 2000 VOLTS (CIRCLE); U_2 = 2300 VOLTS

-24-

PART II

BEAM ANALYSIS OF A VELOCITY MODULATED ELECTRON BEAM

L. R. Bloom
H. M. Von Foerster

INTRODUCTION

In Part I it was shown that a deflector system with the described properties would register a velocity change of electrons in an electron beam with an accurately predictable change in its radial deflection. As can be seen on the representations of different deflection patterns (Figs 10 11 12) a change in radial deflection of about 3% is measurable. Since, for beam voltages of 1500 volts the relative velocity sensitivity σ is at the maximum about 2 (see Eq (18) and Fig 5) an energy modulation of about 1 5% could just be observed

Fortunately there was a velocity modulating device in the laboratory theoretically completely described and experimentally studied and calibrated. Reference is made to the so called "Concentric Line Power Meter" reported in detail in Progress Report No 13. Section 5, of this contract. This device was built especially to have a calibrated velocity modulated electron source at hand for cross checking devices with velocity sensitivity. Since this modulator produces a controlled energy modulation U_{ac}/U_o of about 10% with ease the so produced velocity modulation should be clearly observable with the deflecting system in question

The experiments performed with this modulator will be reported in section 3 of this Part of the report. In the first two sections the results to be expected ill be briefly discussed

1   THE MODULATOR[*]

The modulator essentially consists of a concentric line through
which a thin hole is drilled radially. Through this hole an electron
beam is injected which will be velocity modulated if power is trans-
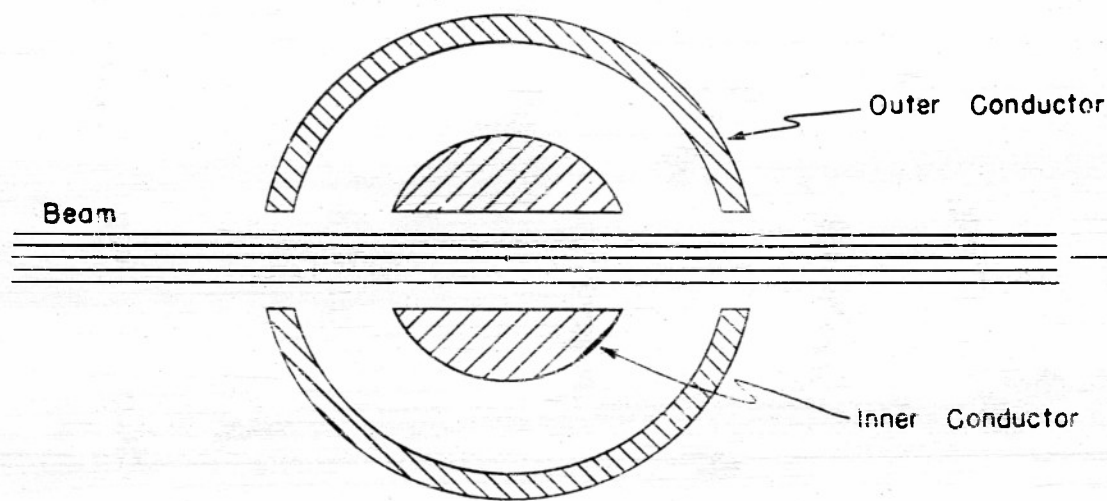mitted through the line. (See Fig. 13.)

FIGURE 13   CONCENTRIC POWER METER   SCHEMATICALLY

It can be shown that the electron beam injected at a voltage U_o
will leave the system energy modulated

$$U = U_o + U_{ac} \sin \varphi_o \tag{31}$$

where the ac component is dependent upon the geometry of the concentric
line and also upon the dc beam voltage U_o and the power P_m flowing
through the line. For a given system

$$U_{ac} = \frac{1}{2} \cdot \sqrt{P_m} \; \psi \, (U_o) \tag{32}$$

and the function $\psi \, (U_o)$ is the simultaneous solution of two transcen-
dental equations. The ψ-function is experimentally well confirmed with a
retarded field method and plotted in Fig. 14.
Since the power flowing through the coaxial line can be measured
easily with a terminating power meter the beam voltage U_o can be
adjusted all quantities in Eq. (32) are given and U_{ac} for any given
condition can be determined. A plot of the expected values of U_{ac} as a
function of P for different U_o is presented in Fig. 15.

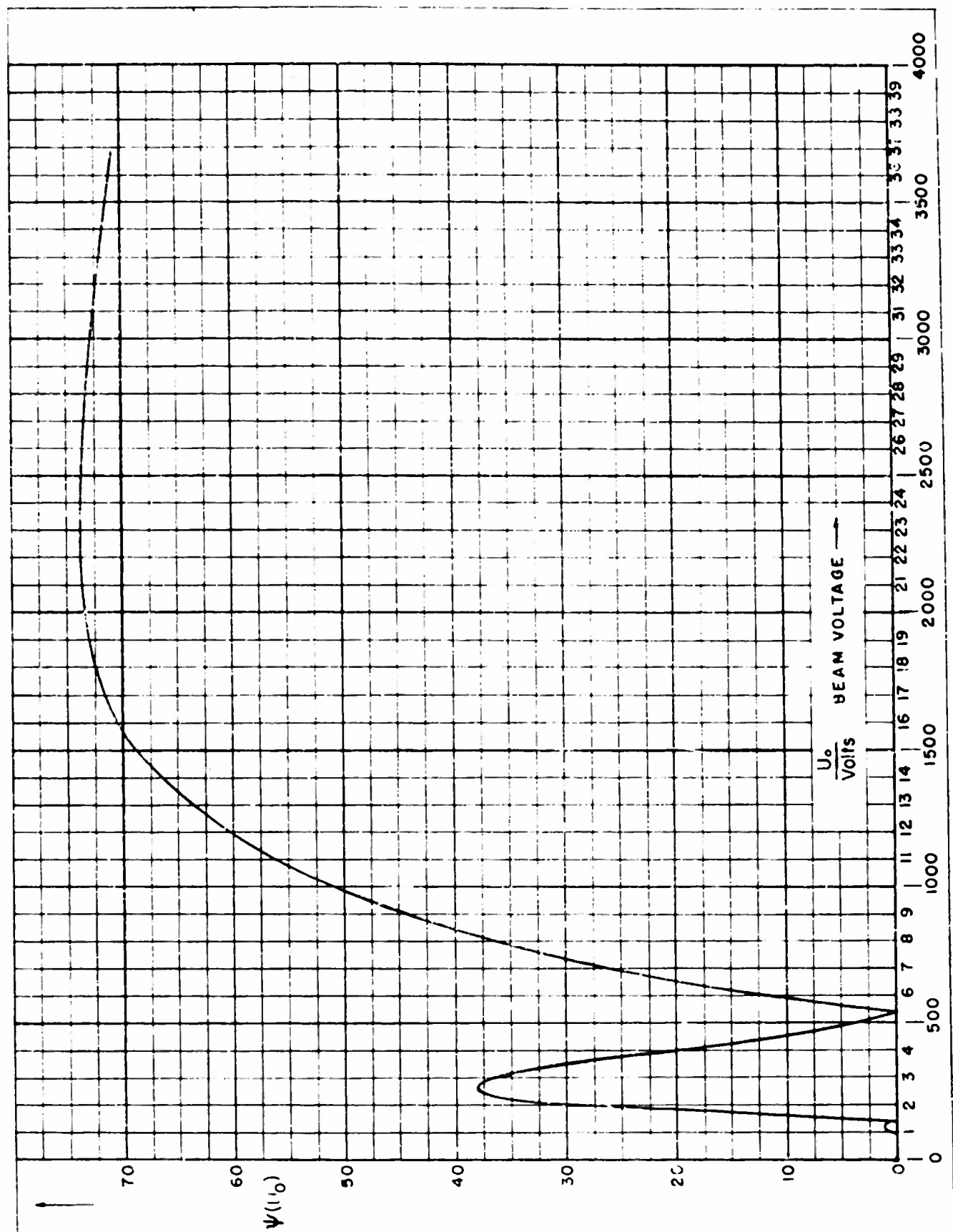[*]For a more extensive description see Progress Report No. 13 N6-ori-71 Task XIX Section 5

FIGURE 14   COUPLING FUNCTION ... ... CENTRE LINE POWER METER
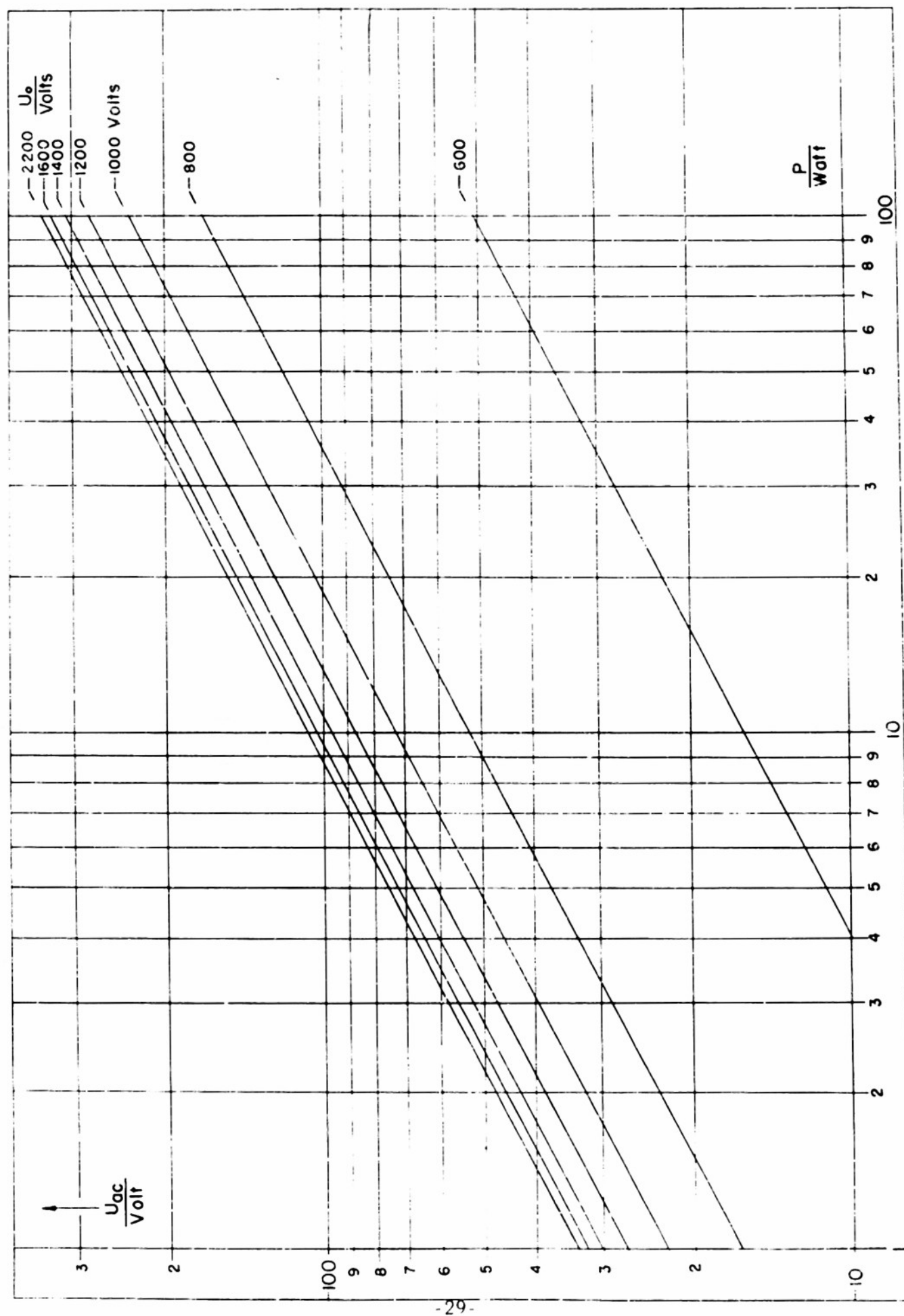
FIGURE 15   a-c COMPONENT OF THE ELECTRON BEAM AFTER BEING MODULATED BY THE CONCENTRIC POWER METER

2   FIRST ORDER BUNCH THEORY

In order to interpret the experimental results presented in the next section properly a brief review of the fundamental concepts of the velocity modulation processes will be given here.*

Suppose there are two devices a modulator and a deflector Both are considered as representable by a plane and shall be a distance of S centimeters apart (See Fig 16)
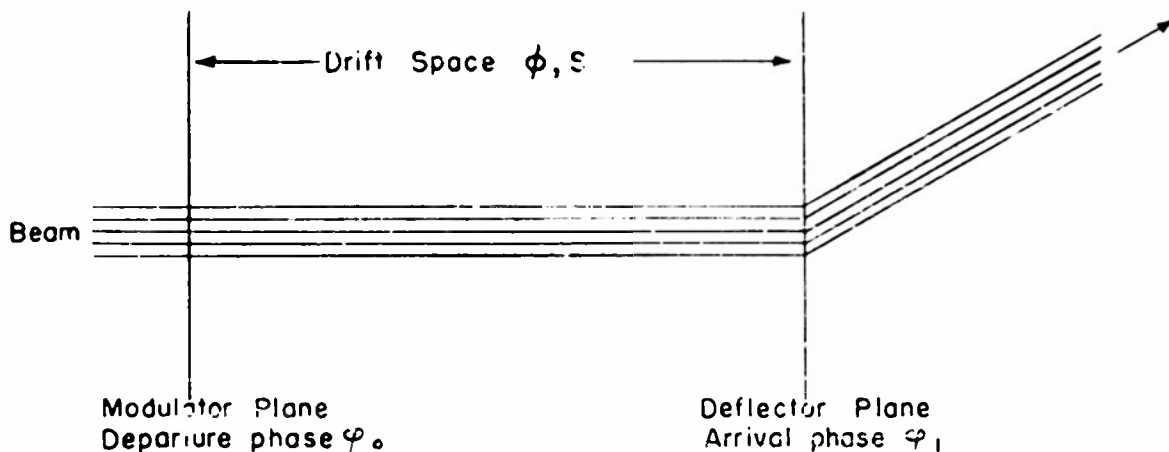

FIGURE 16   MODULATOR DEFLECTOR   SCHEMATICALLY

The modulator is supposed to inject an energy modulated electron beam into the drift region where electrons departing from the modulator plane at a phase angle φ_0 have an energy of

$$U = U_0 + U_{ac} \sin \varphi_0 \tag{31}$$

The first order expression for the velocity of electrons with departure phase φ_0 will be

$$v = v_0 \left(1 + \frac{1}{2} \frac{U_{ac}}{U_0} \sin \varphi_0\right) . \tag{33}$$

Electrons departing at φ_0, after traveling the distance S. will arrive at the deflector plane at an arrival phase φ_1 which is given by

$$\varphi_1 = \varphi_0 + \phi \tag{34}$$

where

$$\phi = \frac{\omega S}{v U} \tag{35}$$

*For a more extensive analysis see   Spangenberg Vacuum Tubes Beck A H N   Velocity
Modulated Thermionic Tubes

-30-

with

$$\sqrt{U_S} = \pi \cdot 10^3 \frac{S}{\lambda} \tag{36}$$

U_S represents the beam voltage making the drift space l radians long
Using Eq (31) to express U in Eq (35) expanding the square root and
inserting into Eq (34) the following equation for the arrival phase φ_1
expressed in terms of the departure phase φ_0 is obtained

$$\varphi_1 = \varphi_0 + \varphi_0 - k \sin \varphi_0 \tag{37}$$

where

$$\varphi_0 = \frac{\cdot \overline{U_S}}{\sqrt{U_0}} \tag{38}$$

and

$$k = \frac{1}{2} \frac{U_{ac}}{U_0} \varphi_0 \tag{39}$$

The expression k usually denotes the "bunching parameter"
Plotting arrival phase φ_1 against departure phase φ_0 for different
bunching parameters k curves of the following form are obtained
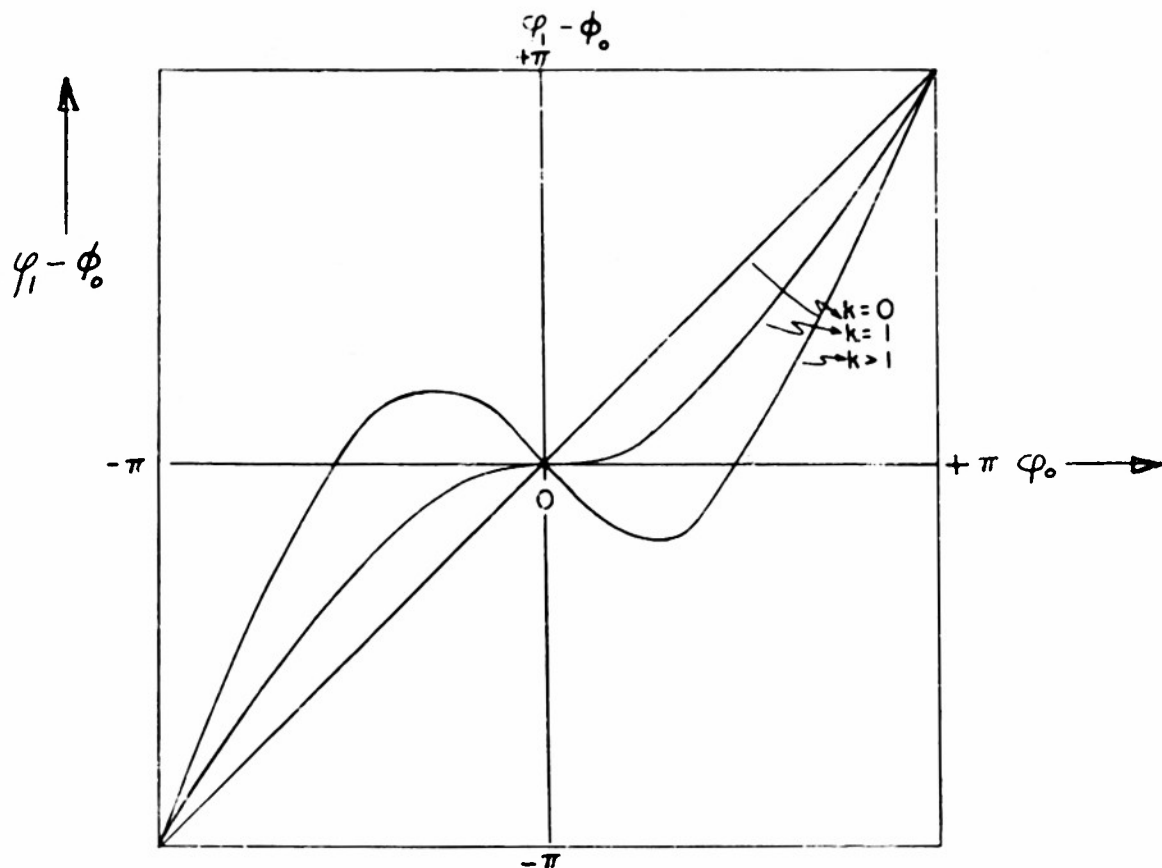

FIGURE 17   ARRIVAL PHASE AS A FUNCTION OF DEPARTURE PHASE
FOR DIFFERENT BUNCHING PARAMETERS k

Application of the principle of conservation of charge for each corres
ponding departure and arrival phase element

$$|\rho_0 \, d\varphi_0| = |\rho_1 \, d\varphi_1| \tag{40}$$

defines the beam density at the deflection plane ρ_1 relative to the
unmodulated density ρ_0 to

$$\frac{\rho_1}{\rho_0} = |\frac{d\varphi_0}{d\varphi_1}| = |(\frac{d\varphi_1}{d\varphi_0})^{-1}| \quad . \tag{41}$$

Differentiating Eq (37) one gets

$$\frac{\rho_1}{\rho_0} = |\frac{1}{1 - k \cos \varphi_0}| \quad . \tag{42}$$

A "bunch" is usually defined if ρ_1/ρ_0 goes to infinity   This is the
case if

$$\cos (\pm\varphi_0^{\bullet}) = \frac{1}{k} \tag{43}$$

Eq (43) has solutions for $k \geq 1$ only   Thus, a single bunch will occur
at $k = 1$ and a double bunch for $k > 1$ These bunches will show up at
the deflector plane at phases which are dictated through Eq (37)
Inserting from Eq (43)

$$\varphi_0^{\bullet} = \pm \arccos \frac{1}{k}$$

into Eq (37), one obtains

$$\varphi_1^{\bullet} = \phi_0 \pm (\sqrt{k^2 - 1} - \arccos \frac{1}{k}) \tag{44}$$

In the deflector plane the arrival phase φ_1 will be converted into a
geometrical deflection angle θ Thus the two bunches expressed in
Eq (44) will appear on the screen as being separated by an angle
$\Delta\theta^{\bullet}$ $\varphi_{11}^{\bullet} - \varphi_{12}^{\bullet}$ This bunch separation angle becomes

$$\Delta\theta^{\bullet} = 2(\sqrt{k^2 - 1} - \arccos \frac{1}{k}) \tag{45}$$

and is plotted in Fig 18   With increasing k, the separation angle will
increase until $\Delta\theta^{\bullet}$ becomes $n \cdot 2\pi$ ($n = 0$ 1 2 3......)   At those
points the two bunches will reunite and again form a single bunch
Solutions for k for the "single bunch condition" are

$$K = 1 \, 00 \quad 4 \, 60; \quad 7 \, 75 \quad 11 \, 00, \quad 14 \, 12 \quad 17 \, 30 \, . \, . \, \pi(n+\tfrac{1}{2})$$
$$n \geq 6 \tag{46}$$

A graphical representation of the bunching process can be given by
using the identity suggested in Eq (41)   Since the first differential

-32-
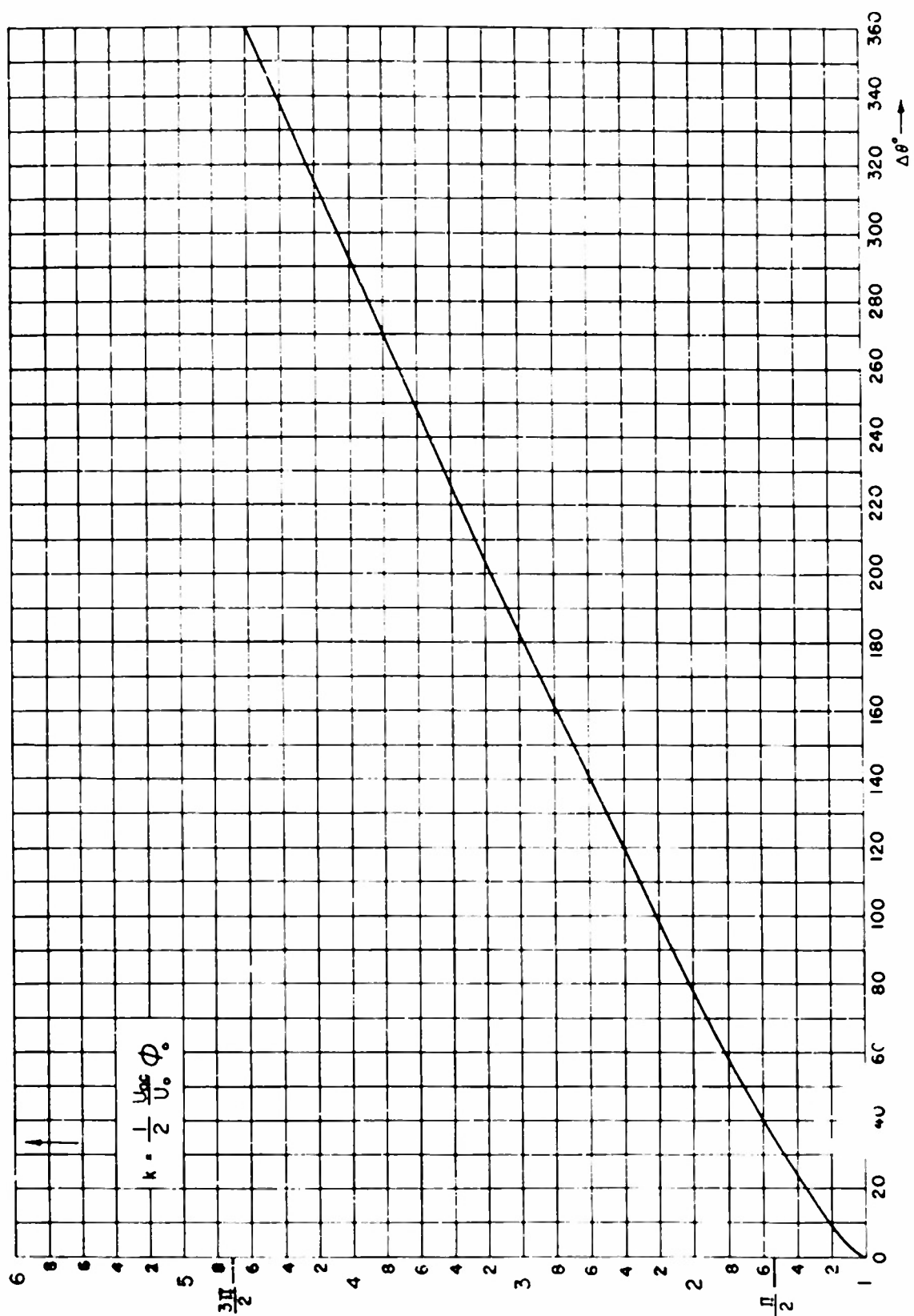
Bunch Separation Angle as a Function of the Bunching Parameter k

Figure 18

$$k = \frac{1}{2} \frac{U_{ac}}{U_o} \phi_o$$

quotient is the tangent of the slope of a curve at the point in question one can get from Eq (41)

$$\frac{\rho_1}{\rho_0} = \left|\frac{d\varphi_0}{d\varphi_1}\right| = \frac{1}{\left|\dfrac{d\varphi_1}{d\varphi_0}\right|} = \frac{1}{|\tan \alpha|} = |\cotan \alpha| = |\tan(90 - \alpha)| = |\tan(\beta)|$$

where α is the slope of the functions connecting φ_1 with φ_0 and shown in Fig 17 In other words. Fig 17 has only to be turned around 90° to obtain a representation of φ_0 as a function of φ_1 where the tangent of the slope β of those curves now directly express the density as a function of the phase angle at the deflector This is drawn schematically in Fig 19

In the diagram in the left upper corner the ac velocity distribution at the modulator plane is plotted It produces for k > 1 a $\varphi_0(\varphi_1)$ diagram presented in the upper right corner (Compare with Fig 17) To obtain the density along the φ_1 axis the three branches of this curve are separately differentiated and the result is shown in the middle section The occurance of the bunches and the significance of the bunch separation angle become evident In the lowest diagram the velocity distribution for the deflector plane is drawn

The construction of this diagram can be carried out by projecting the velocity distribution at the modulator over the $\varphi_0(\varphi_1)$ diagram along the φ_1 axis In other words the velocity of all those electrons which started at different phases φ_{0i} but arrived simultaneously at the deflector at φ_1 are plotted over each arrival angle φ_1 Knowing their departure angle φ_{0i} their velocity is found by tracing back to the velocity distribution curve at the departure plane

It should be noted that for the region between two bunches electrons with three distinctive velocities occur Outside of the bunches each phase element will contain only electrons with the same velocity

To compute the ac velocity distribution at the deflector the departure phase φ_0 must be expressed in terms of the instantaneous ac velocity component Calling the instantaneous ac energy u_{ac} Eq (31) yields

$$u_{ac} = U_{ac} \sin \varphi_0 \tag{47}$$

Solving for φ_0 and inserting into Eq (37) the desired function is found

$$\varphi_1 - \phi_0 = \arcsin \mu - k\mu \tag{48}$$

where

$$\mu = \frac{u_{ac}}{U_{ac}} \tag{49}$$

The velocity distribution at the deflector plane is computed for two different values of k (k = 1 and k 1 37) Since at the deflector plane the phase angle φ_1 is immediately converted into a geometrical
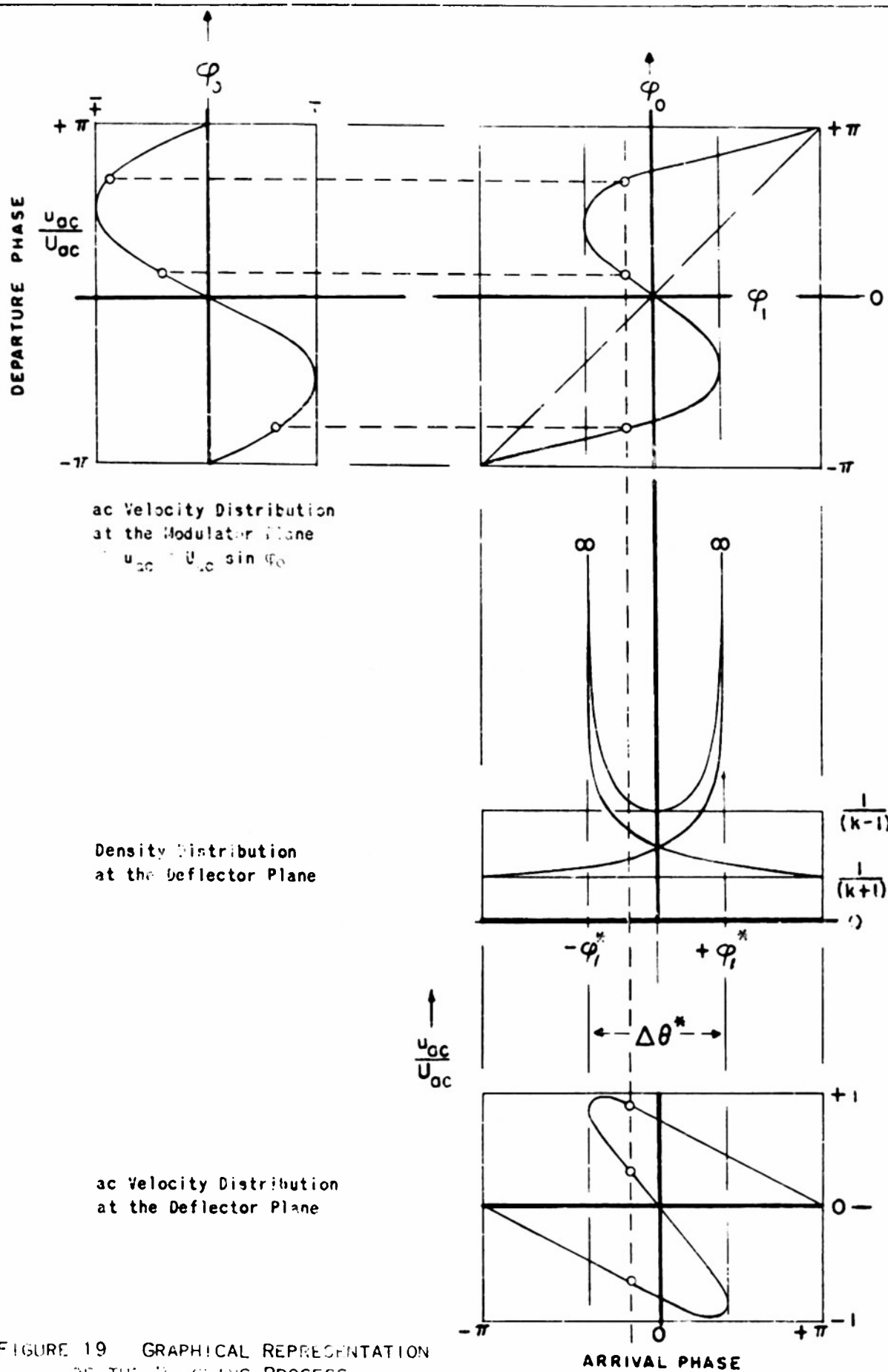
DEPARTURE PHASE

φ_0

$+\pi$

$\dfrac{u_{ac}}{U_{ac}}$

φ_0

$+\pi$

φ_1

0

$-\pi$

$-\pi$

ac Velocity Distribution
at the Modulator Plane
$u_{ac} = U_{ac} \sin \varphi_0$

∞ ∞

Density Distribution
at the Deflector Plane

$\dfrac{1}{(k-1)}$

$\dfrac{1}{(k+1)}$

0

$-\varphi_1^*$ $+\varphi_1^*$

$\dfrac{u_{ac}}{U_{ac}}$

$\Delta\theta^*$

ac Velocity Distribution
at the Deflector Plane

$+1$

0

$-\pi$ 0 $+\pi$

-1

FIGURE 19   GRAPHICAL REPRESENTATION
OF THE BUNCHING PROCESS

ARRIVAL PHASE

deflection angle θ, μ can be plotted in the radial direction along the azimuth θ (See Figs 20 and 21) This representation corresponds closely to what one would expect from the response of the deflector system since electrons with different energies will be projected onto the observation plane at different radii

Finally it may be noted that it can be shown with Eqs (37), (42) and (48) that where a velocity inflection occurs there is also the locus of a bunch
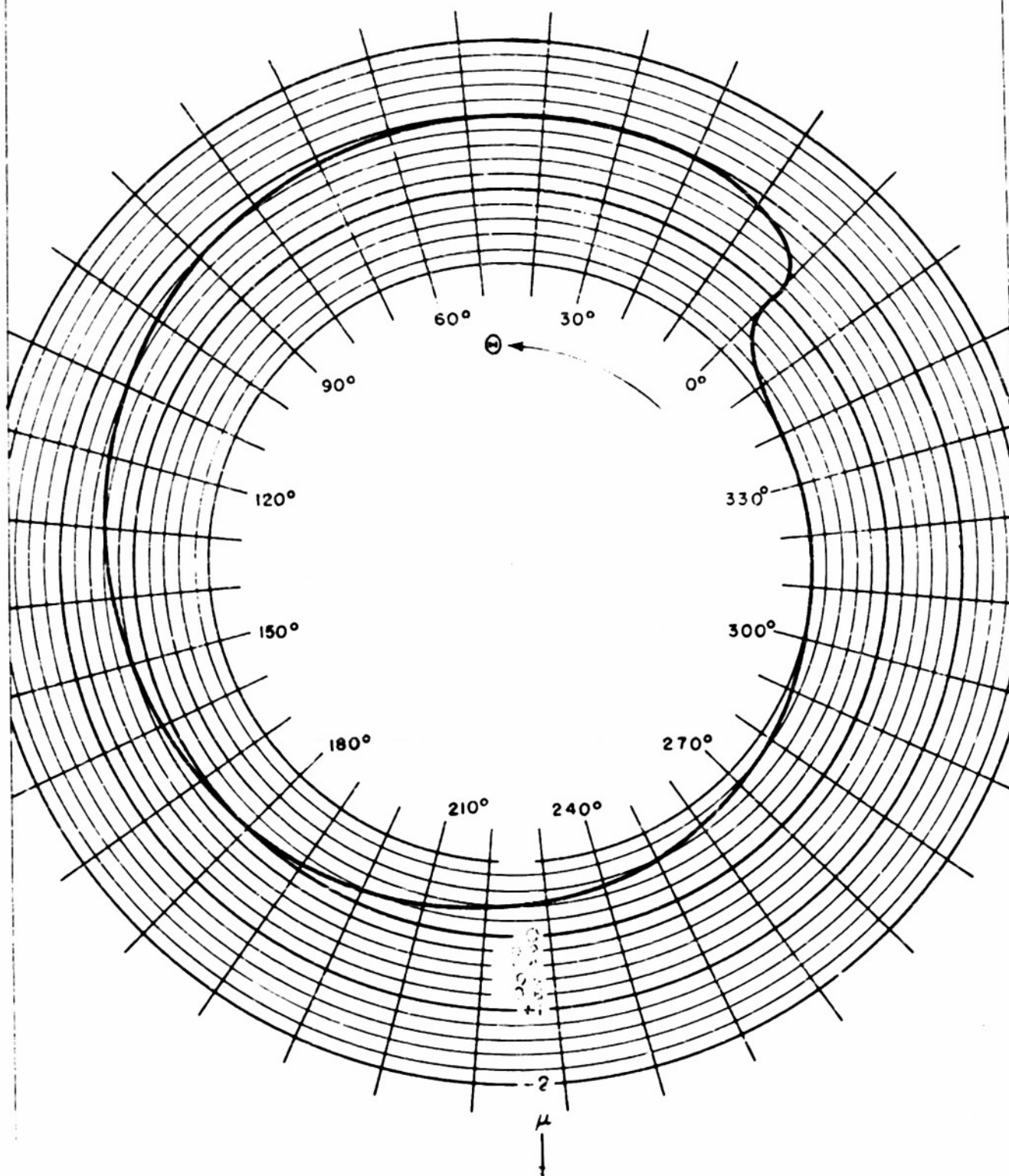
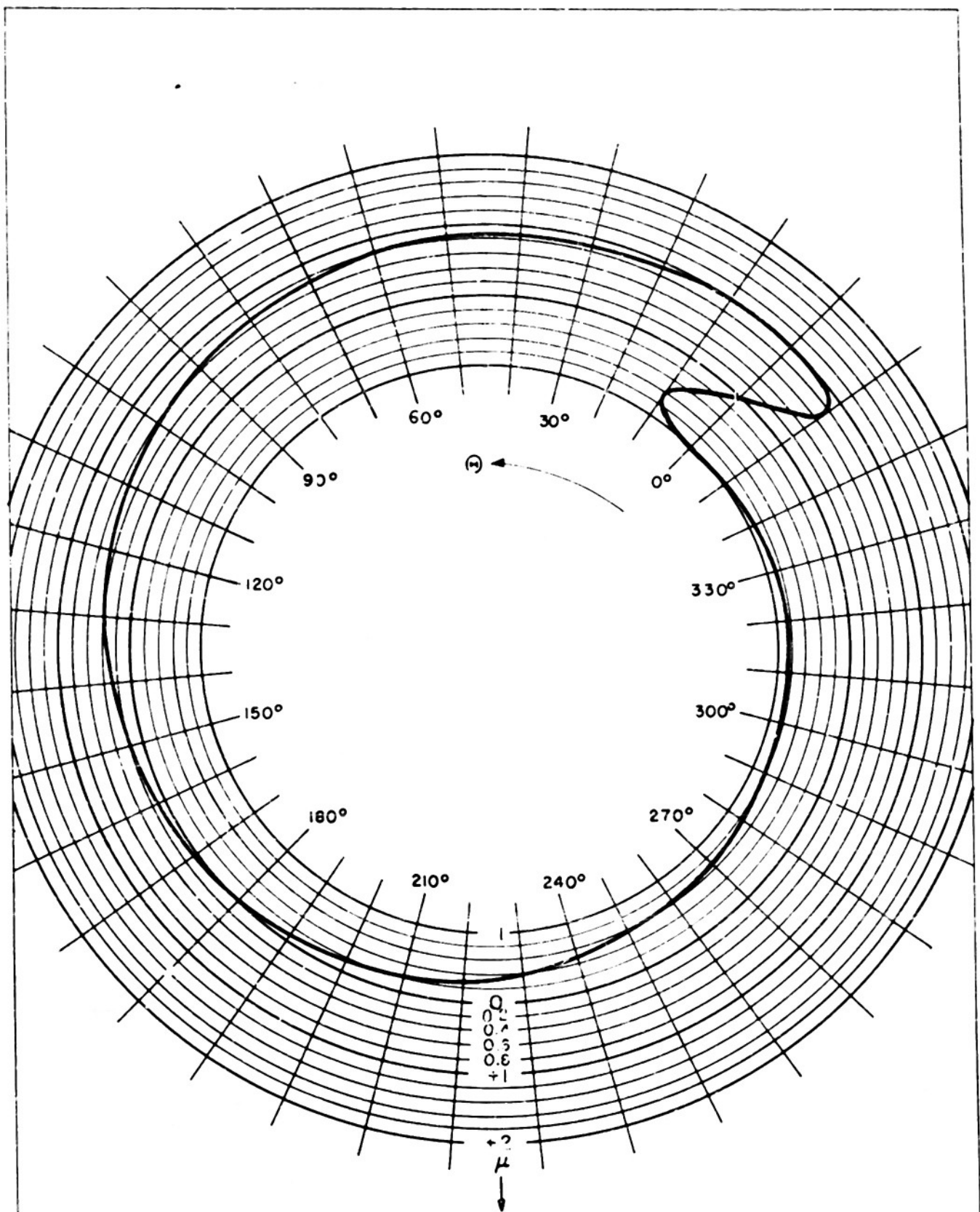FIGURE 20   VELOCITY DISTRIBUTION ALONG THE PERIOD AT n = 1.00

FIGURE 21   VELOCITY DISTRIBUTION ALONG ONE PERIOD AT k = 1.37

3   OBSERVATION OF THE BUNCHING PROCESS

Among the experiments carried out to study the velocity modulation process, the direct observation of the formation of the first bunch and its partition into double bunches by increasing the bunching parameter k was considered to be the most interesting

The experimental setup is described in detail in Part III   Schematically the arrangement is drawn in Fig ___   All systems are reduced to planes
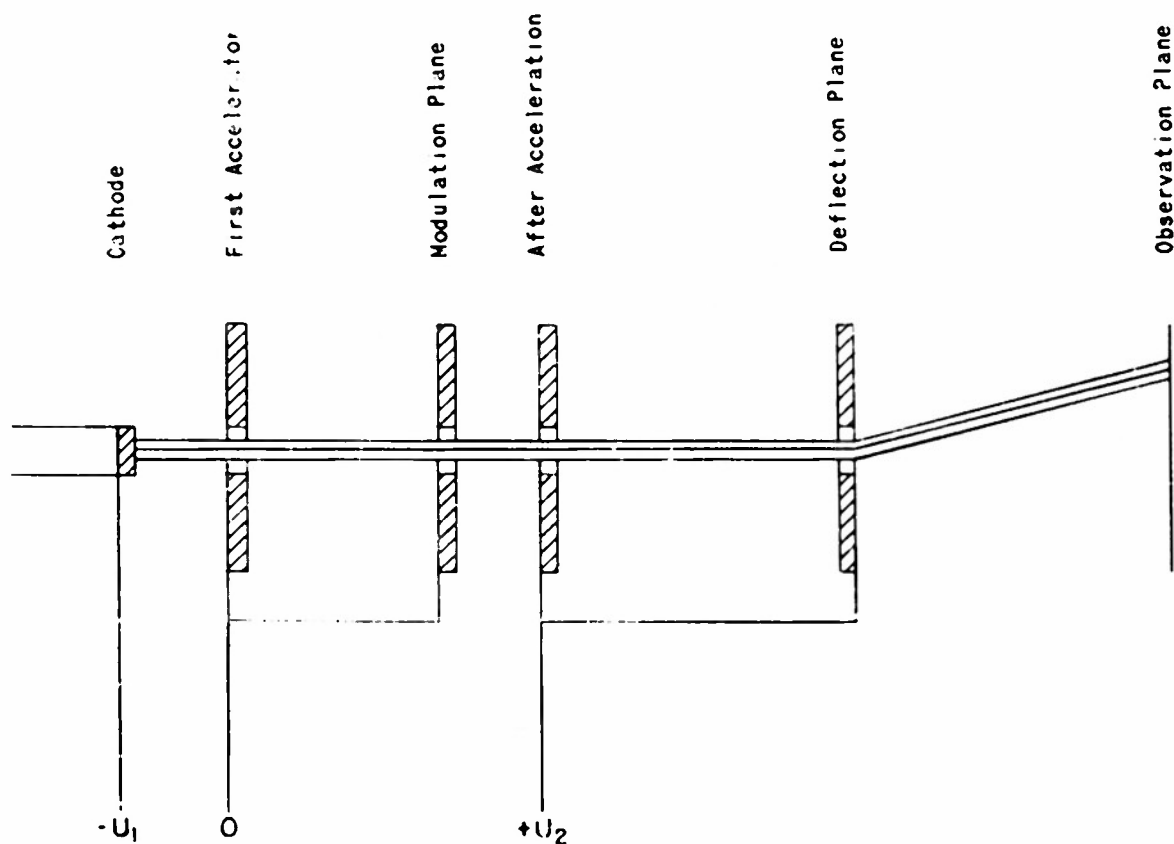
FIGURE 22   EXPERIMENTAL SETUP   SCHEMATICALLY

After the coaxial modulator a post accelerating system was introduced to serve two purposes first to obtain a good focus on the screen independent of the focusing properties of the first accelerator which is usually focused on the modulator plane and second to obtain a wide variability of the drift region between modulator and deflector by varying U_2 without changing the injector voltage U_0 One thus avoids dependence on the variation of the coupling function $\psi(U_0)$ which in turn determines the ac energy component of the beam (See Eq (32) and Fig 14)

Applying the law of the preservation of energy at the velocity jump after the modulator*

$$U = U_0 + U_1 + U_{ac} \sin \tau_0 \tag{50}$$

one obtains with Eqs (32) (36) (38) and (39) the bunching parameter k expressed in quantities which can be controlled from outside alone

$$k = \frac{\pi}{4} \cdot 10^3 \; \psi(U_1) \; \sqrt{P_m} \; \frac{S}{\lambda} \; (U_1 + U_2)^{-3/2} \tag{51}$$

λ was given by the oscillator to be used and S the distance between modulator and deflector was chosen to be 17 cm With

$$S = 17 \text{ cm}$$
$$\lambda = 10 \; 51 \text{ cm}$$

k can be expressed in electrically adjustable quantities

$$k = 1 \; 285 \cdot 10^3 \; \psi(U_1) \; \sqrt{P_m} \quad (U_1 + U_2)^{-3/2} \tag{52}$$

In other words k can be varied during an experiment by varying the injector voltage U_1 or the post acceleration voltage U_2 or the power P_m delivered into the modulator

Since the bunching process should be kept on the most velocity sensitive point namely on the "slow axis" but since a variation of the voltages would necessarily cause a variation of the phase relations within the system it was therefore decided to vary only the power P_m keeping U_1 and U_2 constant Their values were

$$U_1 = 1920 \text{ volts} \qquad U_2 = 1560 \text{ volts}$$

Thus a one to one correlation between k and P_m is established Through Eq (51) and Fig 14 one obtains

$$k = 0 \; 460 \; \sqrt{P_m} \tag{53}$$

Seven values of P_m were chosen and determined the following values of k

$$P_m = 5\;5 \quad 7\;1 \quad 9\;5 \quad 11\;2 \quad 13\;8 \quad 15\;6 \quad 20\;0 \quad \text{watts}$$
$$k = 1\;08 \quad 1\;22 \quad 1\;42 \quad 1\;54 \quad 1\;71 \quad 1\;83 \quad 2\;06$$

*See Appendix II

2.5°
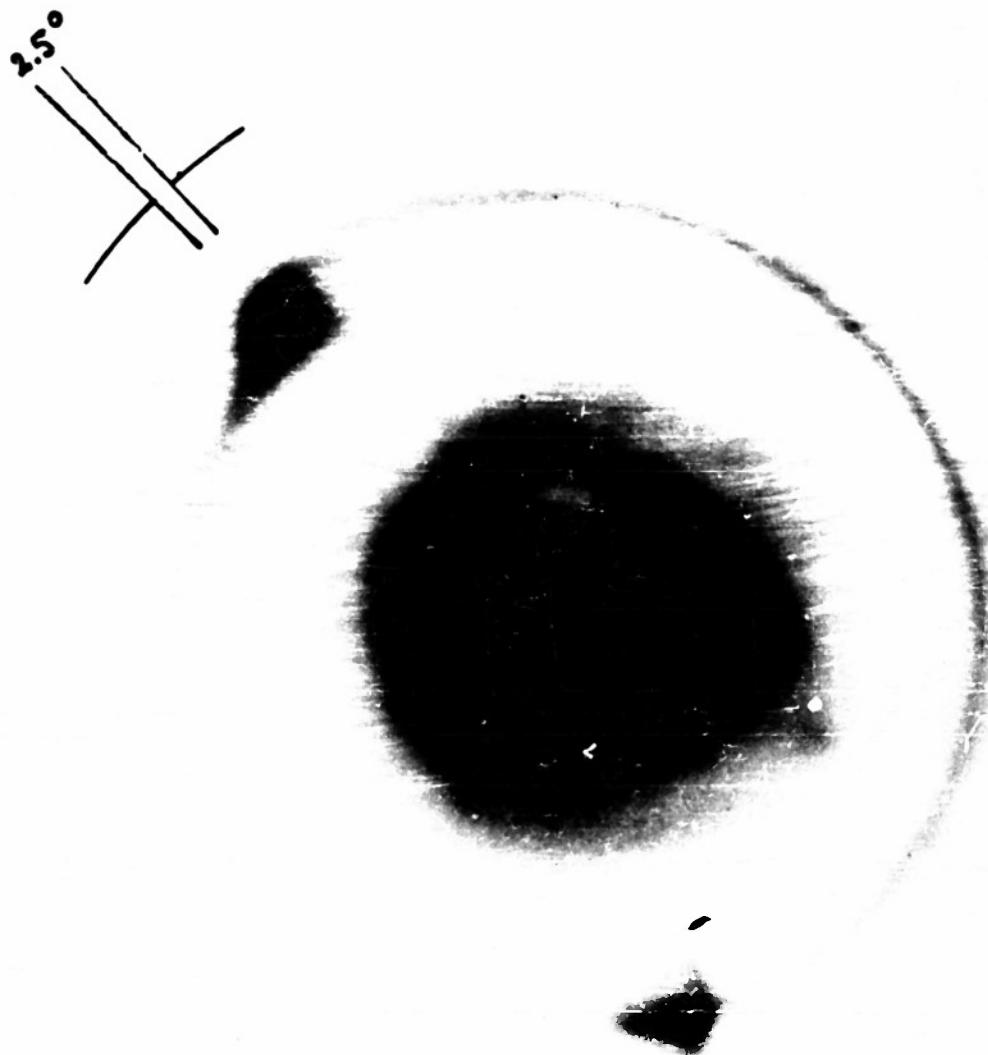
FIGURE 23.1   K = 1.08

$(\Delta\theta^{\circ})_P = 2.5°$ $(U_{ac})_P = 85$ VOLTS

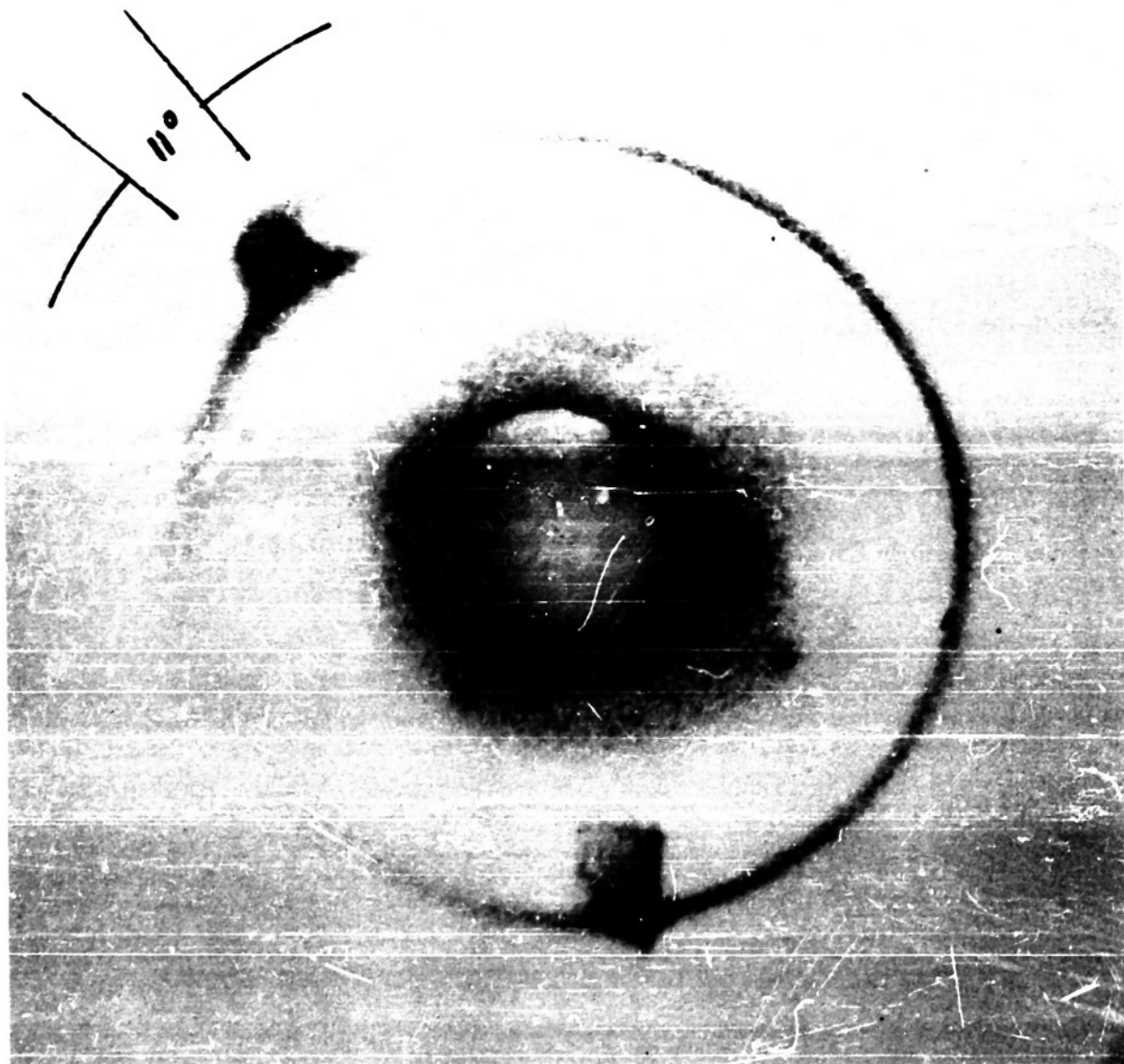$(\Delta\theta^{\circ})_{OBS} = 8°$ $(U_{ac})_{\Delta R} = 110$ VOLTS

FIGURE 23.2   K = 1.22

$(\Delta\theta^*)_P = 11°$ $(U_{ac})_P = 96$ VOLTS

$(\Delta\theta^*)_{OBS} = 10°$ $(U_{ac})_{\Delta R} = 117$ VOLTS
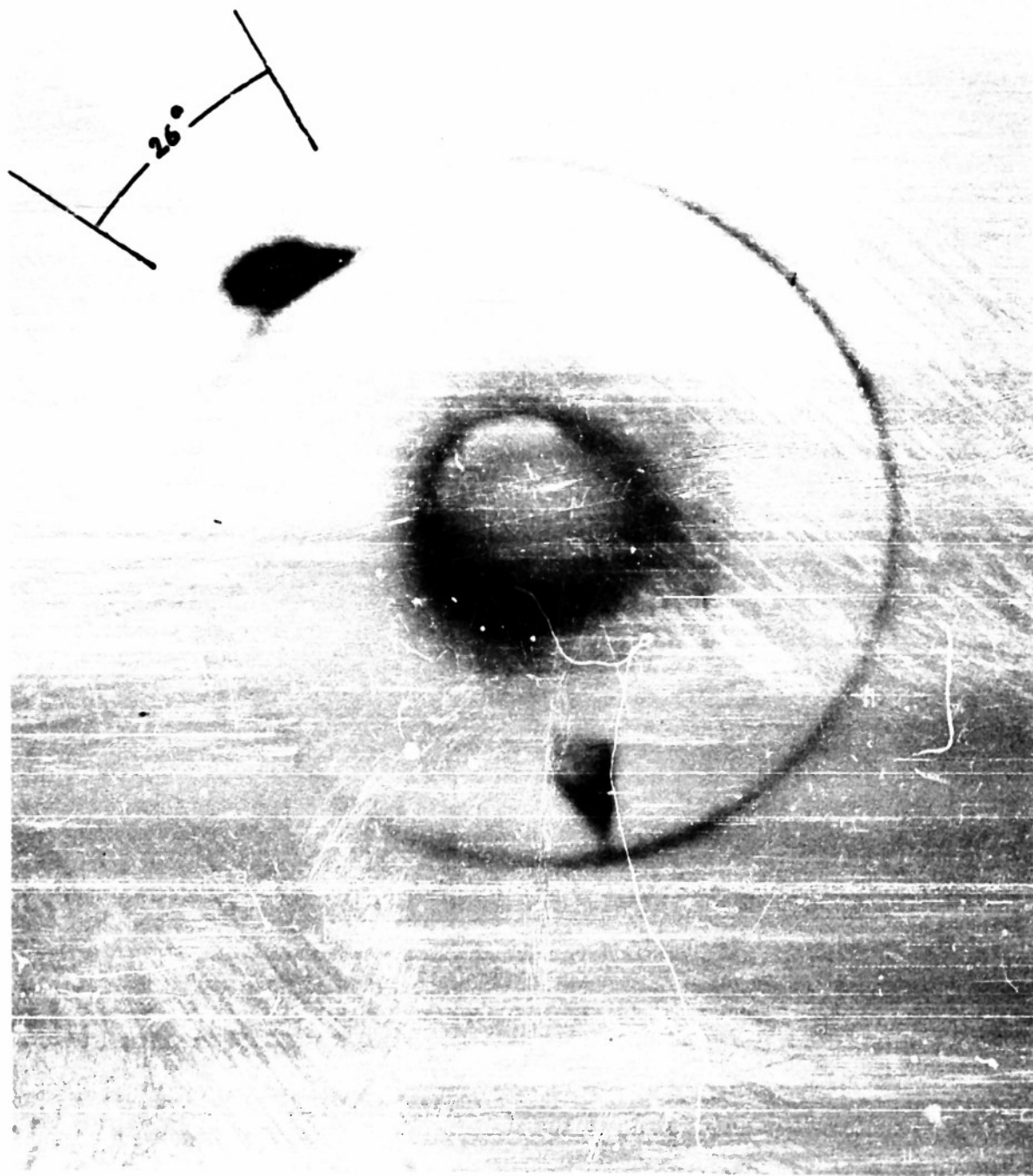
FIGURE 23.3   K = 1.42

$(\Delta\theta^{*})_{?}$ = 26° $(U_{ac})_{P}$ = 112 VOLTS

$(\Delta\theta^{*})_{OBS}$ = 25° $(\underline{U}_{ac})_{\Delta R}$ = 130 VOLTS
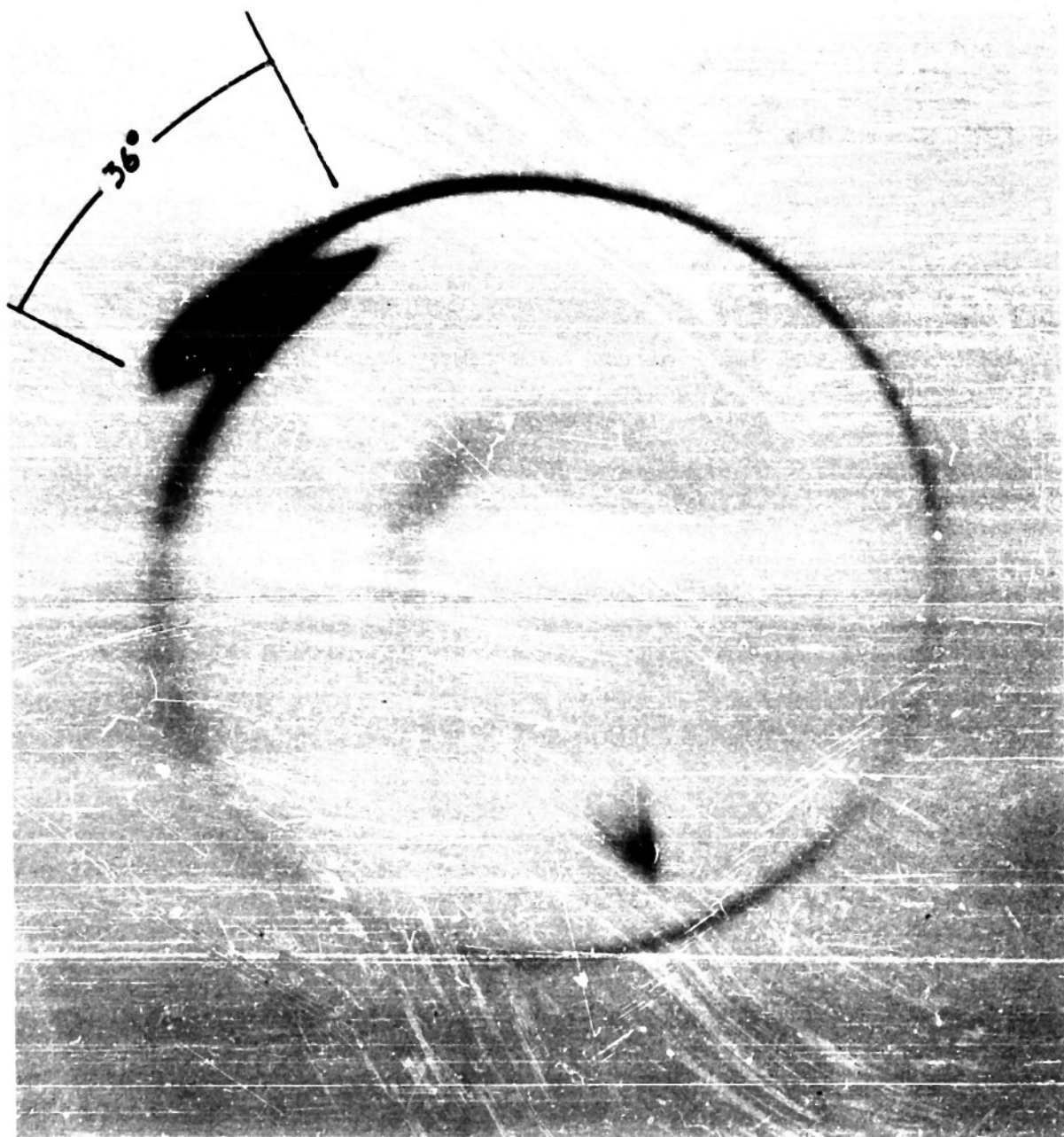
FIGURE 23.4 K = 1.54

$(\Delta\theta^\circ)_P$ = 36° $(U_{ac})_P$ = 123 VOLTS

$(\Delta\theta^\circ)_{OBS}$ = 40° $(\underline{U}_{ac})_{\Delta R}$ = 135 VOLTS

-44-
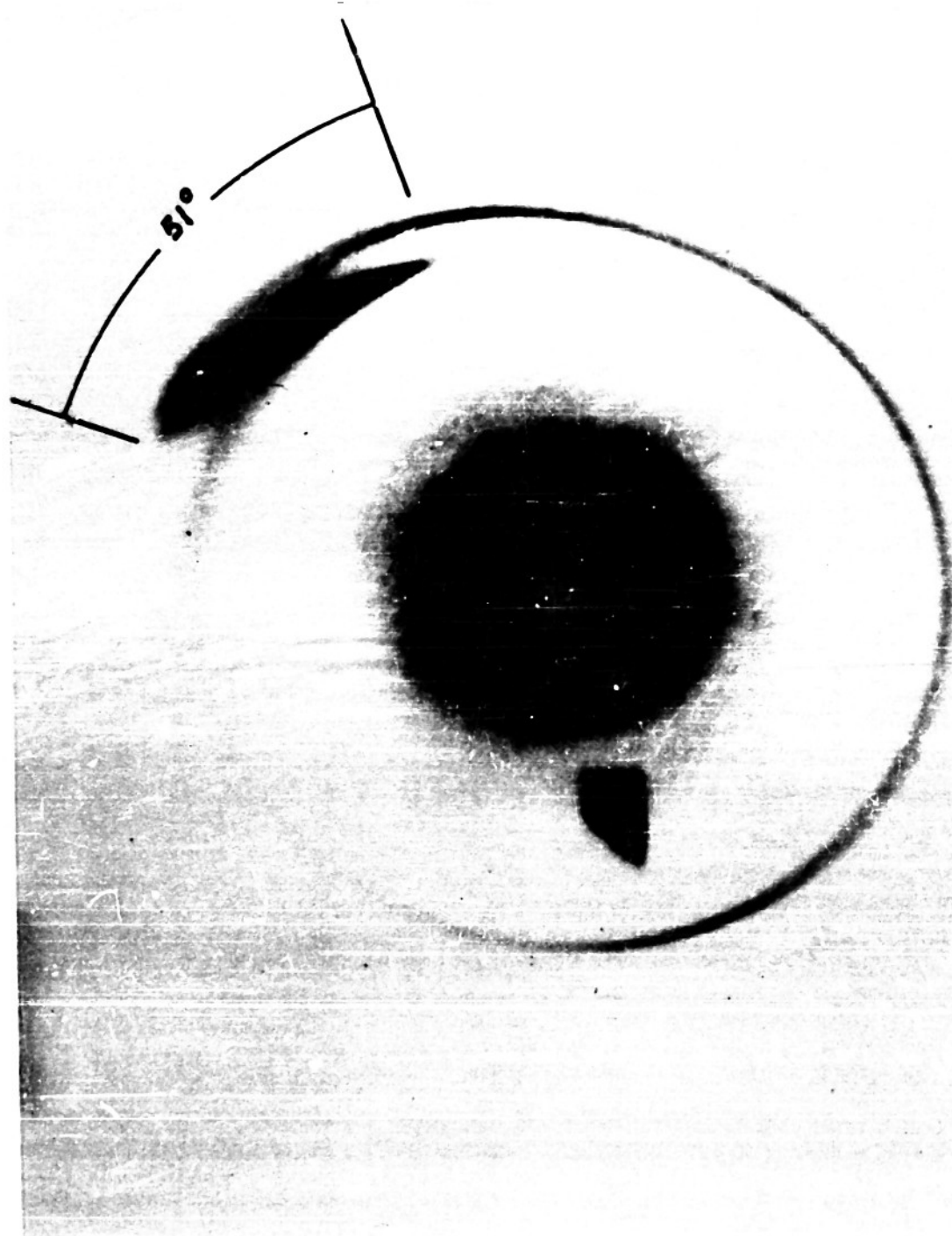
FIGURE 23.5   K = 1.72

$(\Delta\theta^*)_P = 51°$ $(U_{ac})_P = 135$ VOLTS

$(\Delta\theta^*)_{OBS} = 52°$ $(\underline{U}_{ac})_{\Delta R} = 142$ VOLTS
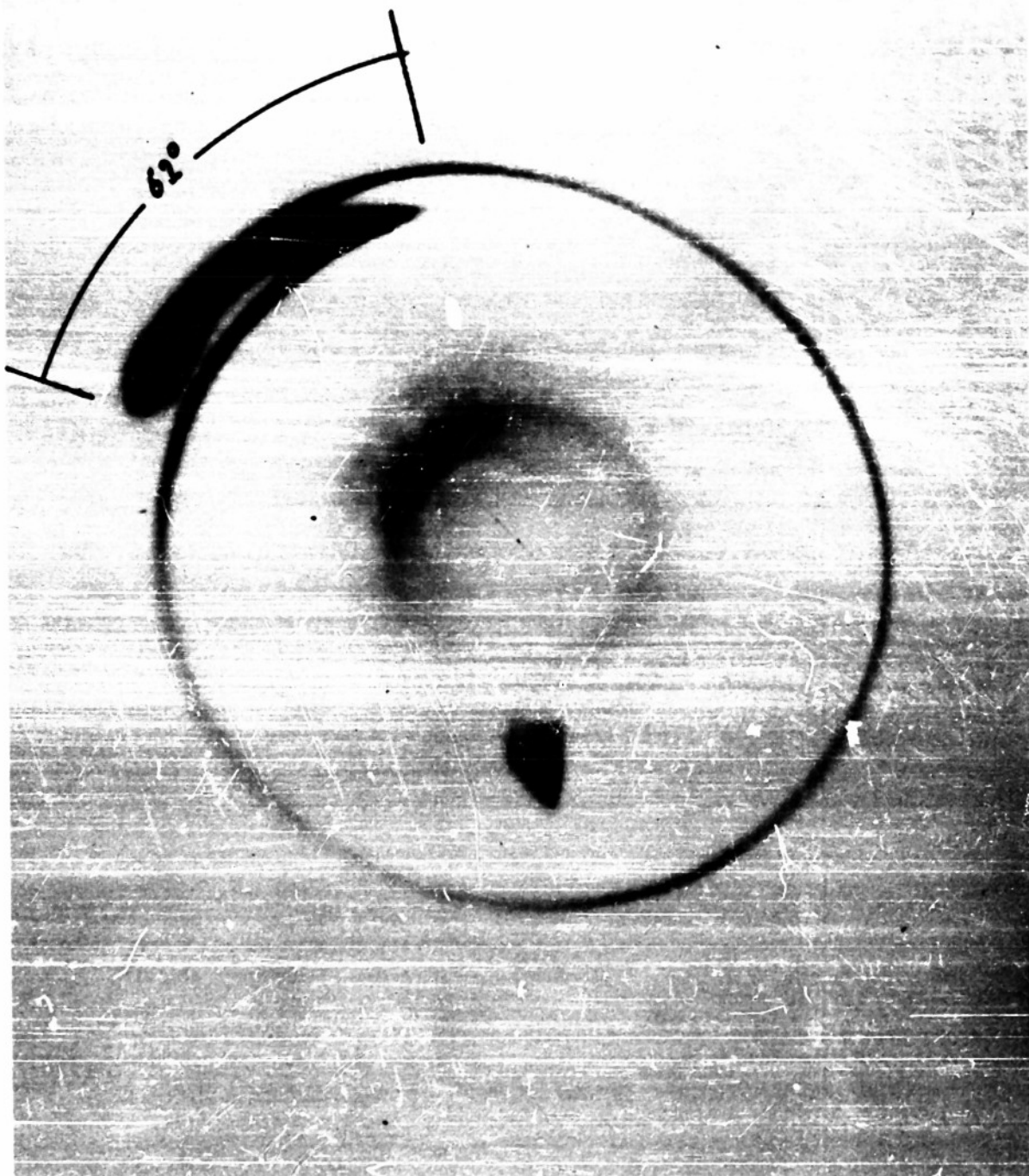
FIGURE 23.6   K = 1.83

$(\Delta\theta^*)_P = 62°$ $(U_{ac})_P = 143$ VOLTS

$(\Delta\theta^*)_{OBS} = 57°$ $(U_{ac})_{AR} = 156$ VOLTS

FIGURE 23.7

$K = 2.06$

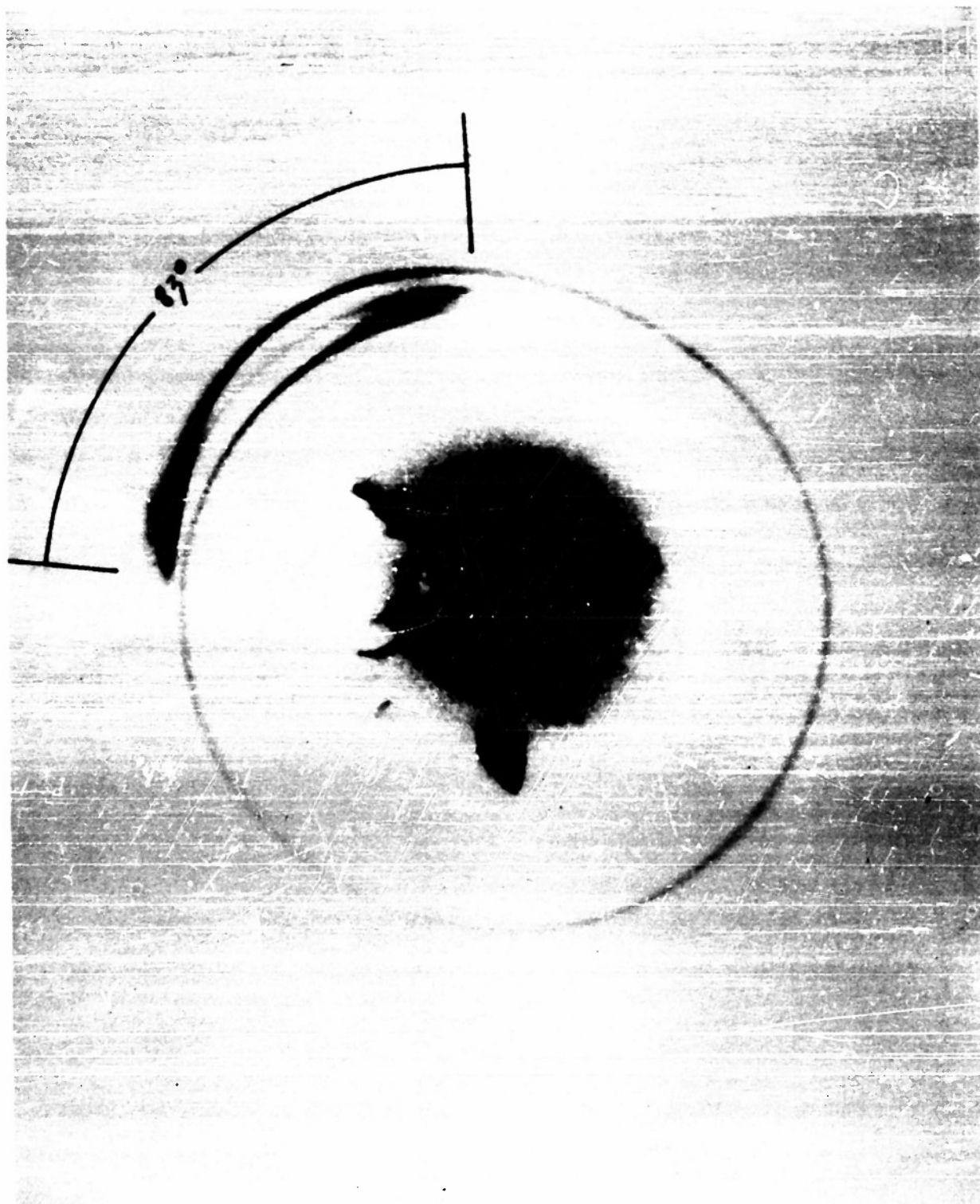$(\Delta \theta^*)_P = 83°$

$(U_{ac})_P = 162$ VOLTS

$(\Delta \theta^*)_{OBS} = 83°$

$(U_{ac})_{OBS} = 180$ VOLTS

-47-

For each value of k a picture was taken and is presented in Figs 23 1 to 23 7

In Fig 23 1 the occurance of the first bunch* which should occur at k 1 is clearly seen The resemblance with the computed μ presen tation for k 1 in Fig 20 is easily noted Again the beam swings clockwise thus Fig 23 1 is a reflection on the y axis of Fig 20 **

Increasing the bunching parameter k the bunch begins to divide itself and the double bunch is clearly presented in Fig 23 4 for k 1 54 Note also the three distinctive velocity groups in the region between the two bunches The bunch separation angle $\Delta\theta^\bullet$ can be computed for a given k through Eq (45) or with Fig 18 This is done in Table I and compared with the observed values of $\Delta\theta^\bullet$ The indices "P" and "obs" indicate by which method these values were obtained The agreement be tween these values is surprisingly good except for the first value, where the bunch should still be a tight spot with a width of only 2 5° This may have several causes which could be properly determined only after a more extensive study of the region around the formation of the first bunch

But the general good agreement of the set of values suggests that the determination of the velocity of the electrons at the modulator was quite accurate Otherwise they would occur at the deflector plane after traveling over the long drift region of about 17 cycles at quite dif ferent phases Thus the double check holds A triple check can be performed by utilizing the velocity sensitivity in the radial direction according to the considerations presented in Part I

Since all the measurements were made with the bunch at the "slow axis' to obtain maximum velocity sensitivity in the radial direction Eqs (19) and (20) are applicable Using these equations U_{ac} is found to be

$$ U_{ac} \quad \frac{\Delta R}{R} \quad \frac{U_1 \cdot U_2}{\sigma_{Slow}} \tag{54} $$

and inserting all known numerical values

$$ U_{ac} = 2560 \quad \frac{\Delta R}{R} \text{ volts} \tag{55} $$

On the other hand U_{ac} can be determined by Eq (32) or if more trust is placed in the precision of the bunching process over the observed $\Delta\theta^\bullet$ by using Eqs (45) and (39) The determination of ΔR had to take the finite beam width into consideration Two values of ΔR were taken the one determined by the open gap between the overlapping beam traces the other by measuring the distance between the center lines of the traces Thus a minimum and maximum value of U_{ac} was defined with Eq (55) Table II compares the three values

* The bunch should not be mistaken for the dark spot at the bottom of the circle This is a light marker to indicate the actual circle radius During the experiment the power was in creased by increasing the power output of the oscillator Since the deflector was fed with a constant fraction of the power delivered to the modulator each setting resulted in a larger deflection thus in an increased circle radius The light marker approaches the center with increasing k because the enlargements were made for constant circle radius

** Figures 20 and 21 do not take into account particular velocity sensitivity in the R di rection μ is plotted radially in arbitrary units With respect to the radial direction therefore these Figures are not intended to give a complete description of the phenomens to be observed

TABLE I

COMPARISON OF THE BUNCH SEPARATION ANGLE $(\Delta\theta^*)_P$ COMPUTED
THROUGH EQ. (45) WITH THE OBSERVED BUNCH
SEPARATION ANGLE $(\Delta\theta^*)_{OBS}$ AS MEASURED ON FIGS. 23.1-23.7

Fig No	$(k)_p$	$(\Delta\theta^*)_p$	$(\Delta\theta^*)_{obs}$
23 1	1 08	2 5°	8°
23 2	1 22	11°	10°
23 3	1 42	26°	24°
23 4	1 54	36°	40°
23 5	1 71	51°	52°
23 6	1 83	62°	57°
23 7	2 06	83°	83°

TABLE II

COMPARISON OF THE ac-ENERGY COMPONENT U_{ac} COMPUTED
THROUGH EQ. (32) WITH THE OBSERVED ac ENERGY
COMPONENT AS MEASURED ON FIG. 23.1 23 7 FROM THE RADIAL SPREAD ΔR

Fig No	P	$(U_{ac})_p$	$(\underline{U}_{ac})_{\Delta R}$	$(U_{ac})_{\Delta R}$
23 1	5 5	85	110	180
23 2	7 1	97	117	170
23 3	9 2	112	130	165
23 4	11.2	123	135	160
23 5	13 8	135	142	175
23 6	15 6	143	156	172
23 7	20.0	162	180	180

The agreement is surprisingly bad This is mainly due to the fact that close to the bunch the determination of the beam width beco. es somewhat unprecise One could now arg that the method of using the radial sensitivity of the deflector to give accurate results has failed since the determination of U_{ac} with the very sensitiv phase method, using $\Delta\theta°$ confirmed the expected values of U_{ac}

On the other hand if one is willing to take the $(U_{ac})_{\Delta R}$ values as real it could be argued that in the phase method the velocity is pro perly measured only between the modulator and shortly before the de flector But the ΔR ... is .... va. .s of the velocities and they can at the moment of the formation of the bunch assume v.lues which may be of the order of the .... ener.y U_{ac} Indeed, the $(U_{ac})_{\Delta R}$ value approaches its expected valu. $(U_{ac})_p$ if the bunches have moved a considerable istance away Figure 24 illustrates this fact where both values of $(U_{ac})_{\Delta R}$ are plotted against $(U_{ac})_p$ The striated region fills out the uncertainty in determining U_{ac} The straight line represents the expected value of U_{ac} without any inter action of the electrons in the bunch

It is not absurd perhaps to think that an interaction between the bunch and the beam electrons t.kes place when the bunches are ploughing their way through the beam with a phase elocity slightly higher and slower than the average electron velocity

A hint that space charge effects may account for this discrepancy, is given by closer inspection of the photographs In Figs 23 5 23.6 and 23 7 an interesting process can be observed namely, the impover- ishment of the electron density in the region between the bunches with pr. ressive partition of the two bunches Theoretically, this region should be much denser or at least comparable with the density along the trace which connects the two bunches the long way around In this connection compare Fig 1. the density diagram with Fig 23 7 One gets the impression that one bunch pushing forward and the other back ward almost sweep the middle section clear of electrons

Only a much more detailed study can finally clear up the different problems remaining at this point However a clear indication of the feasibility of the method was obtained in the very first stages of the experimental work Since there are no fundamental problems in the construction of systems ith much higher radial velocity sensitivities it is hoped that further investigations of this possibility may be made
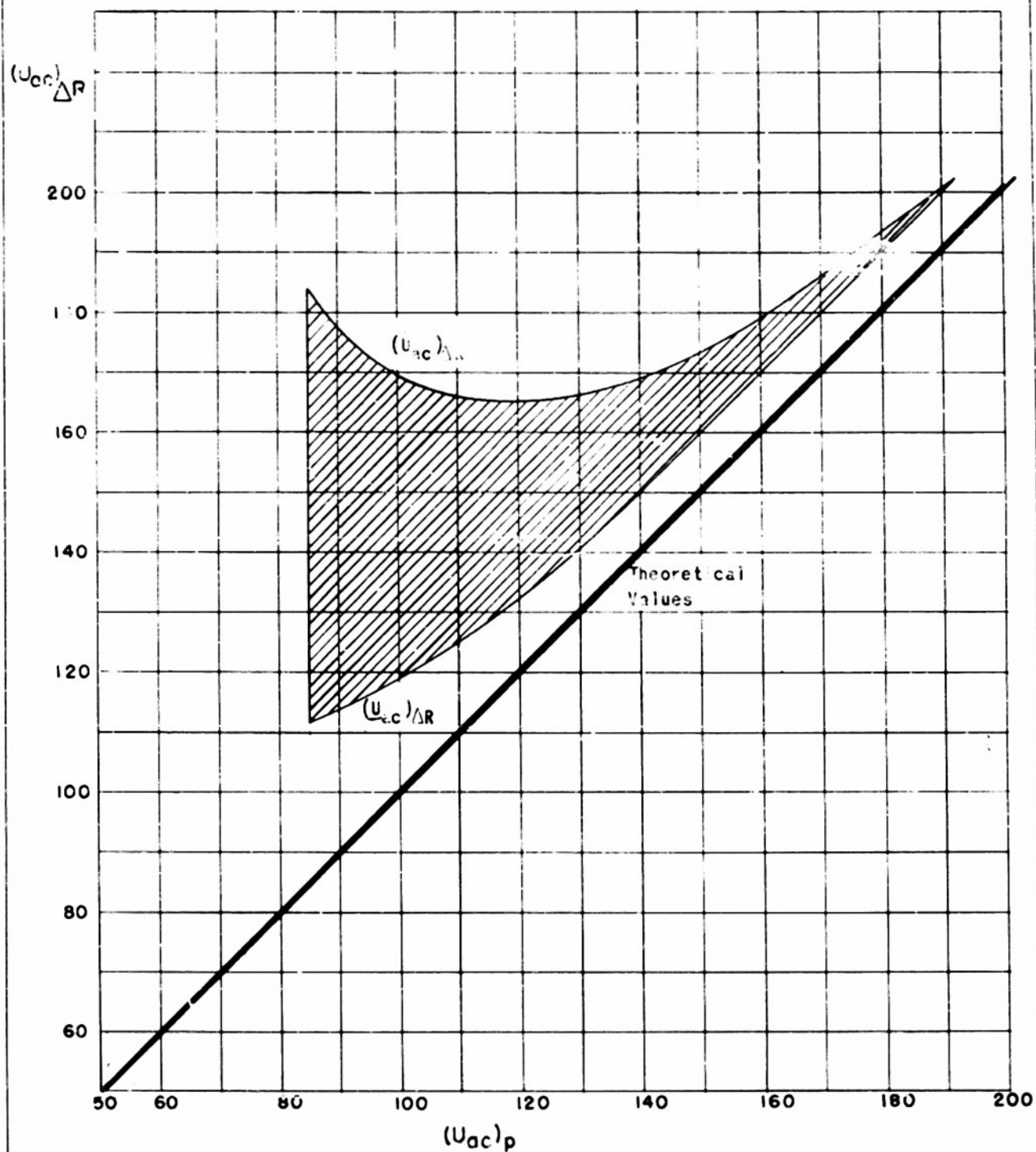
FIGURE 24   ac ENERGY COMPONENT MEASURED ACCORDING TO THE ΔR METHOD
COMPARED WITH THE ac ENERGY COMPONENT AS COMPUTED
ACCORDING TO THE POWER METER READINGS

PART III
THE EXPERIMENTAL SETUP

L.R. Bloom

1   DESCRIPTION OF THE APPARATUS

The general arrangement of the components making up the beam analyzer is given in schematic diagrams Figs 25 and 26 and in the photographs of the assembly Figs 27 and 28 The analyzer essentially consists of three parts

1 The electron beam source under consideration

2 The r f circular deflection system made up of the crossed Lecher wire system and

3 The viewing plane (a cathode ray screen) on which the elements of the beam which have been scattered according to phase and velocity may be studied

The analysis of the deflection system has been presented in detail in Part I Section 1 of this report The constructional details are observable in the drawing and photograph Figs 6 and 7 The spacing between Lecher wires diameters and other constructional data are given in Fig 6 One additional dimension which should be mentioned is the actual length of the Lecher wire line inside the shorting cylinder The length chosen was $L = \frac{\lambda}{2}$ or 5 cms This provides for a maximum voltage to appear between Lecher wires midway between the ends and therefore a maximum deflection of the beam when the Lecher wire line is tuned to resonance

The velocity modulator the operation of which is presented in Part II Section 2 is shown in the drawing Fig 29 and in the photograph Fig 30 A second lens system was mounted immediately beyond the output gap of the velocity modulator to permit post acceleration of the beam In addition a dc parallel plate deflection system was provided to insure that the beam would pass between the wires of the Lecher wire deflection system The total drift length between the output of the velocity modulator and the plane of the first pair of deflection wires was $L = 17$ cm This length was chosen to insure the forming of the first bunch of the beam in the neighborhood of the Lecher wire lines for moderate beam voltages and velocity modulation power

In order to make sure that the modulation frequency and the deflection frequency are the same and to permit phasing of the one system with respect to another it is necessary that both the deflection system and the modulator be driven from a common source *

---

* Although a common oscillator is necessary as indicated it is very desirable to have the amplitude and phase of the r-f signal to each of the component elements independently variable This is discussed further toward the end of this Part

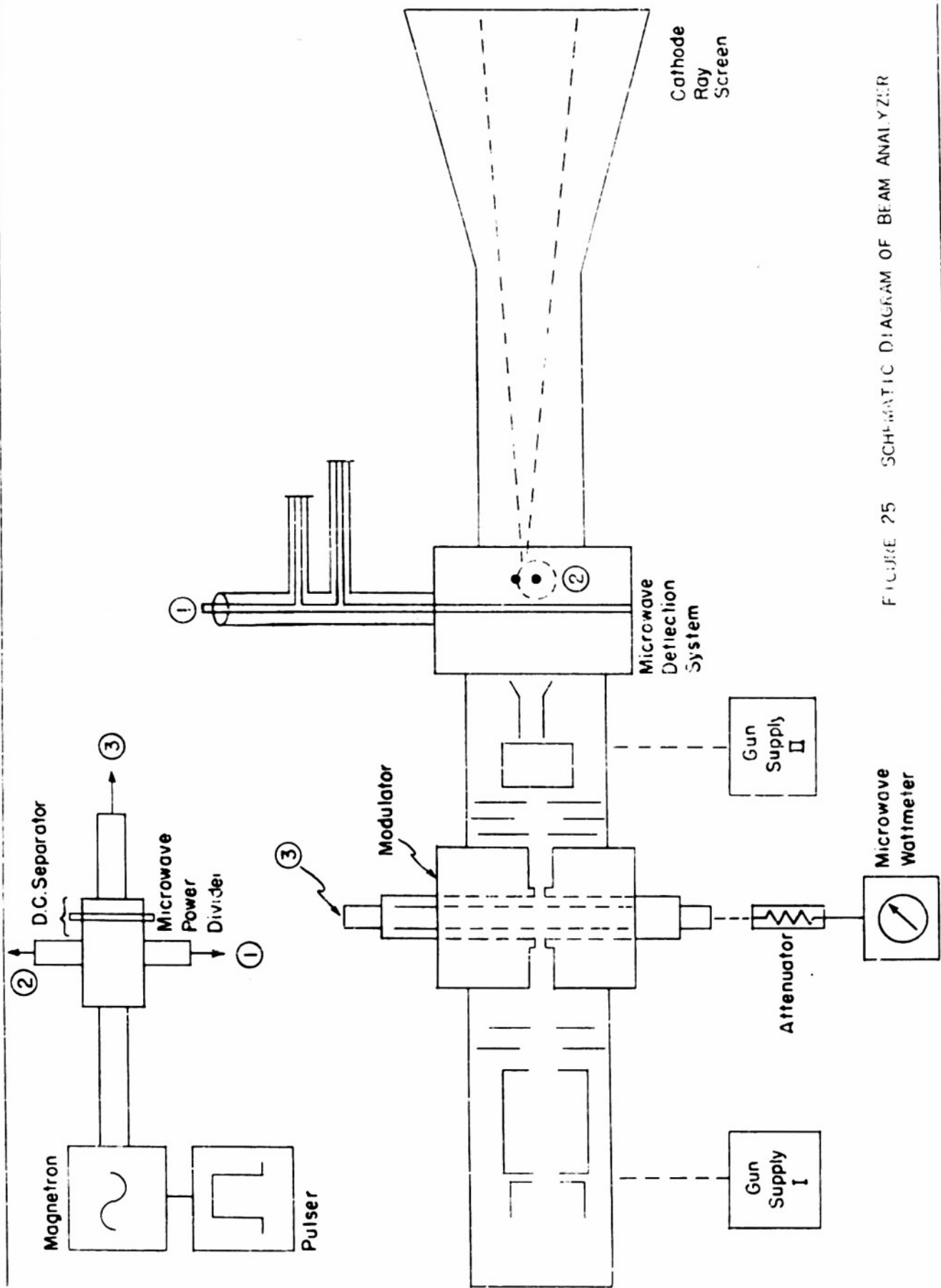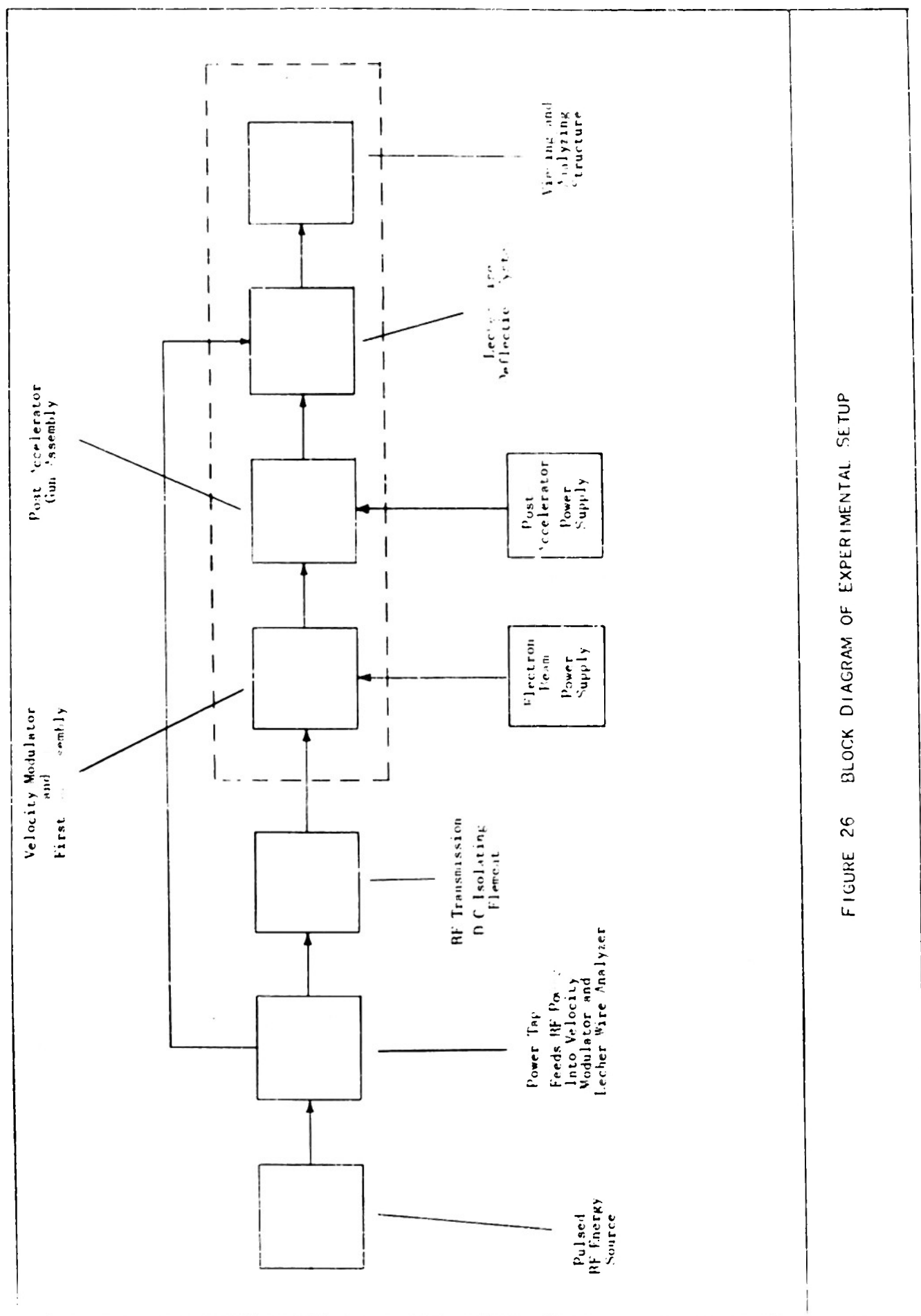FIGURE 25 SCHEMATIC DIAGRAM OF BEAM ANALYZER

- Cathode Ray Screen
- Microwave Deflection System
- Gun Supply II
- Microwave Wattmeter
- Attenuator
- Modulator
- Gun Supply I
- D.C. Separator
- Microwave Power Divider
- Magnetron
- Pulser

Pulsed RF Energy Source

Power Tap Feeds RF Power Into Velocity Modulator and Lecher Wire Analyzer

RF Transmission DC Isolating Element

Velocity Modulator and First ... ...embly

Post Accelerator (Gun Assembly)

Electron Beam Power Supply

Post Accelerator Power Supply

Electron ... ... Reflectic ... ...

Vie ... ... and ... lyzing ... tructure

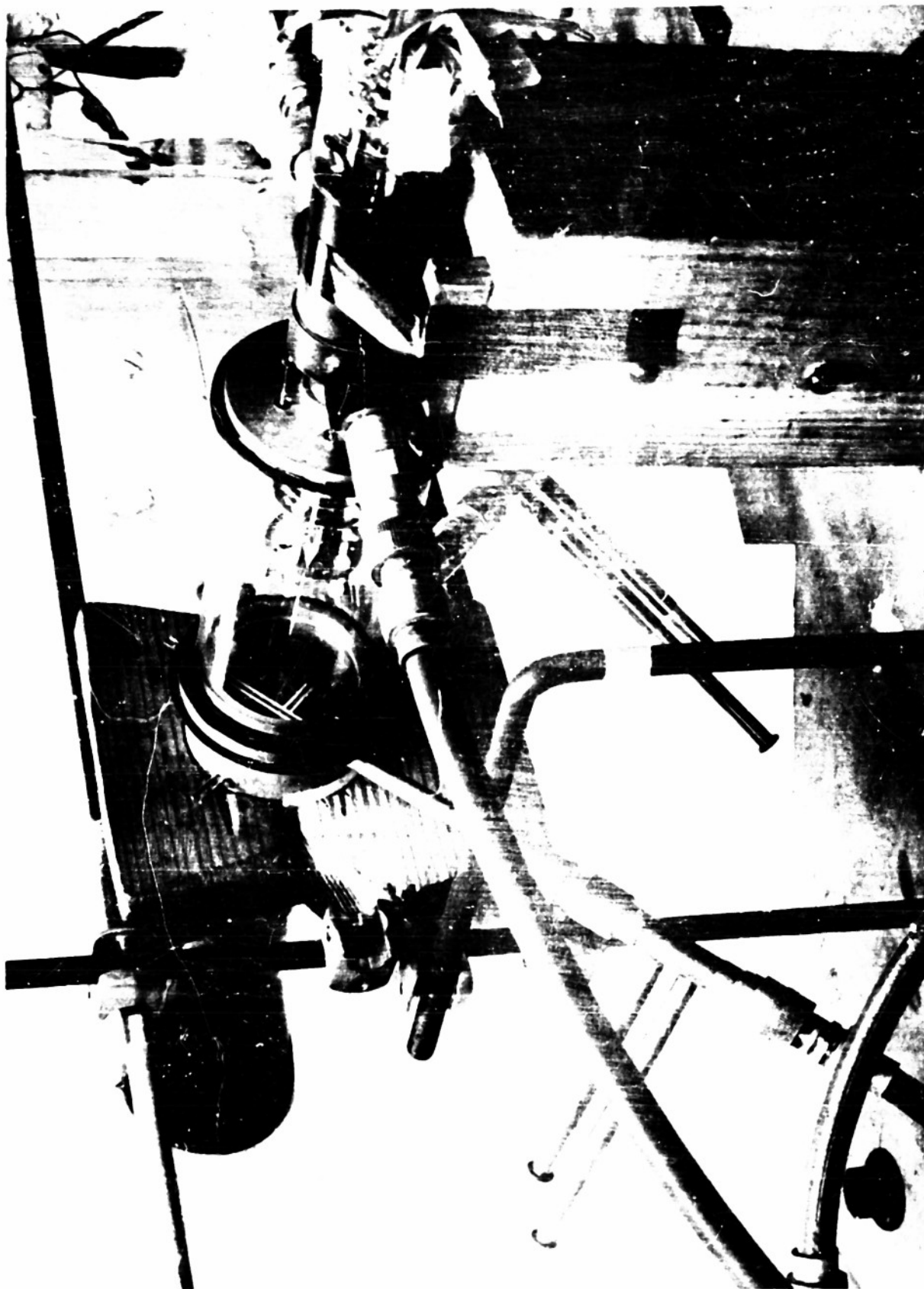FIGURE 26   BLOCK DIAGRAM OF EXPERIMENTAL SETUP
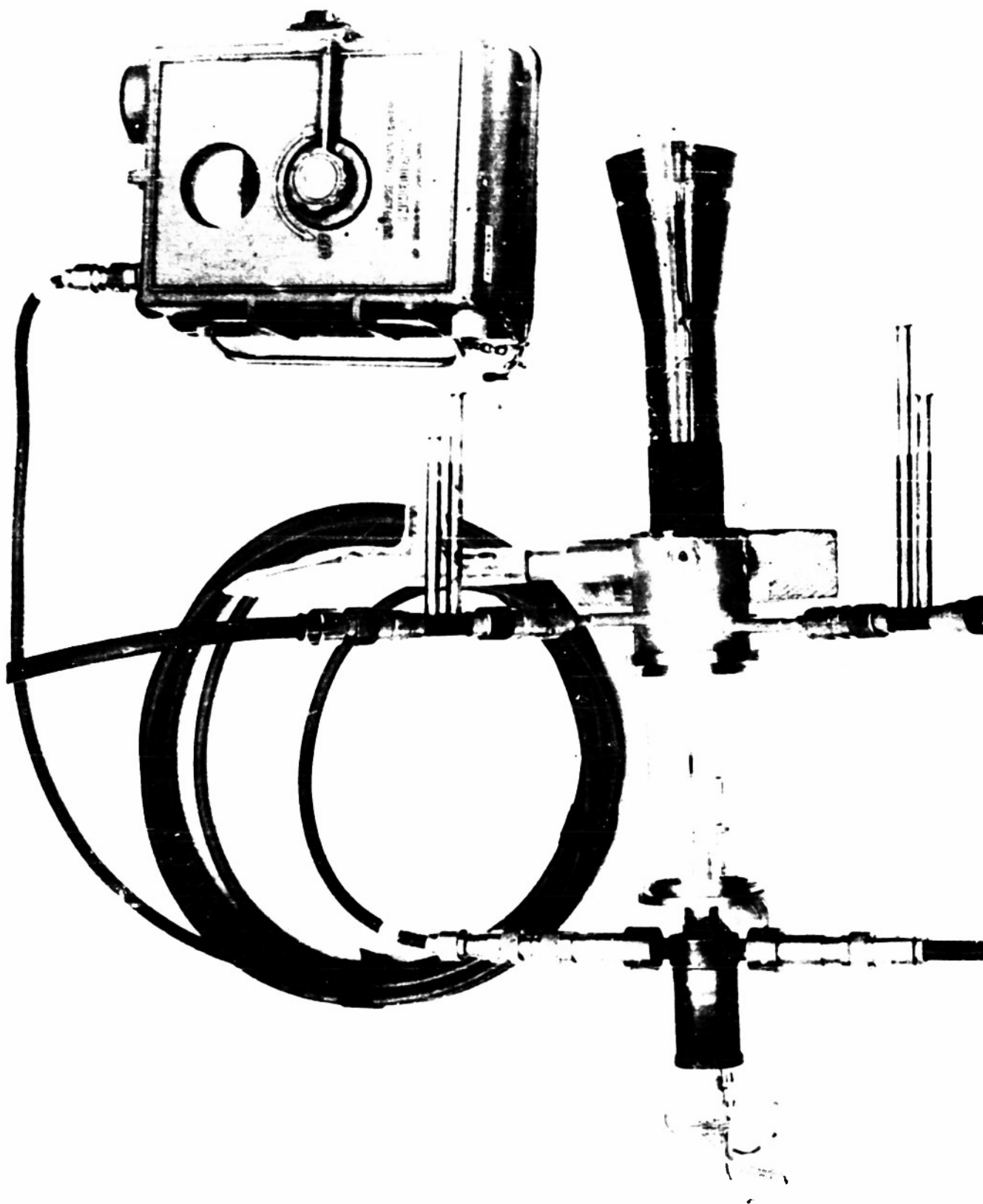
FIGURE 27   BEAM ANALYZER SYSTEM

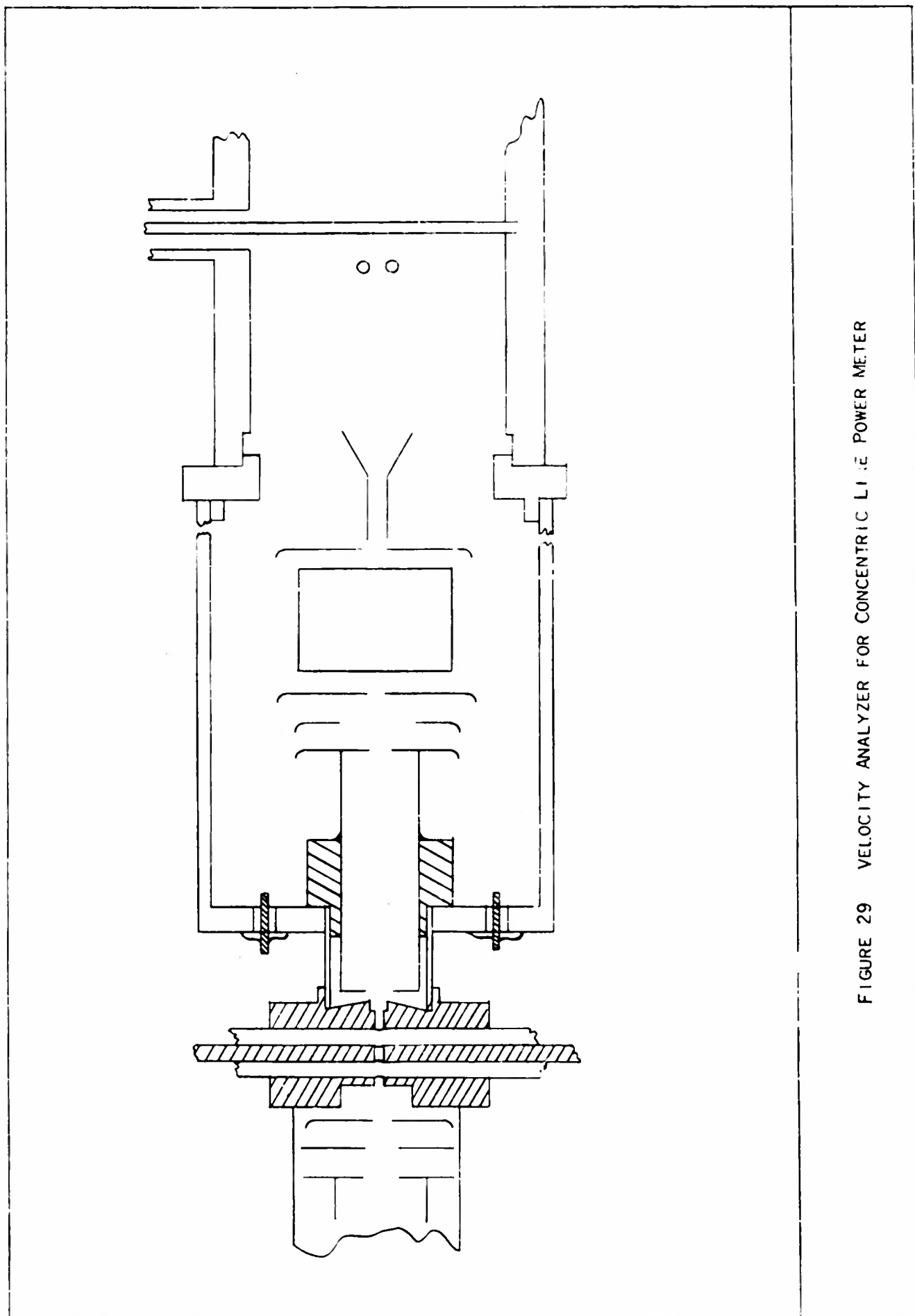FIGURE 28 BEAM ANALYZER ASSEMBLY

FIGURE 29   VELOCITY ANALYZER FOR CONCENTRIC LINE POWER METER
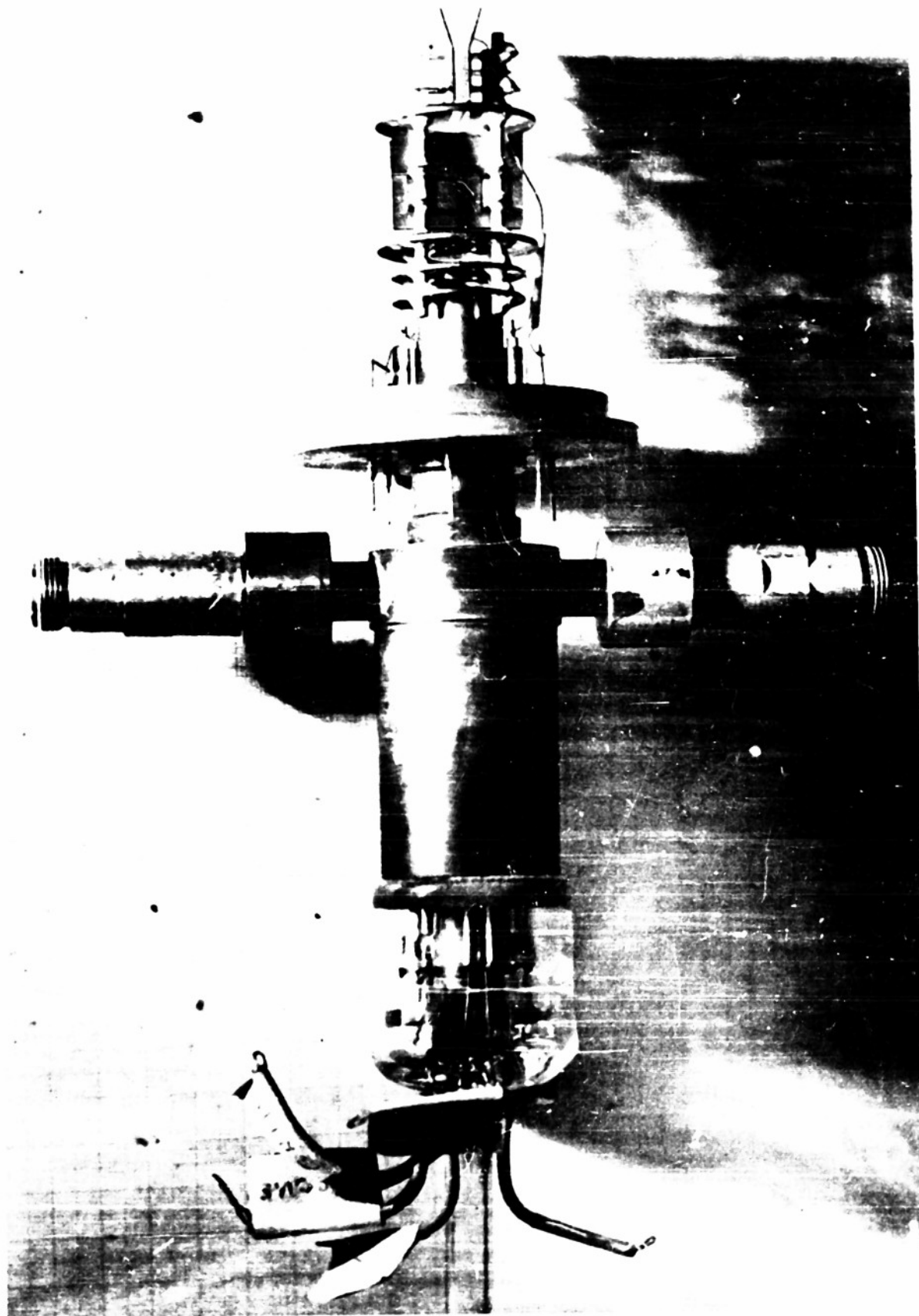
FIGURE 30   MODULATOR AND POST-ACCELERATOR

2   THE MICROWAVE CIRCUIT

The r f generator was a Raytheon QK (59 62) cw type of magnetron,
tunable over a narrow range in the 10 centimeter region   This magnetron
was driven from a pulsed power supply although it could just as well
have been cw operated   The magnetron had been used previously in a set
of experiments which required pulsed operation and for this purpose a
hard tube pulser and power supply had been built which could drive the
magnetron up to 300 watts peak   The pulse duration could be adjusted
from 5 30 micro seconds at a repetition rate up to 5000 times per second
The pulse shape was sufficiently square so that no observable variation
in power occurred during the duration of the pulse   Typical pulse
shapes of the voltage input and the power output of the magnetron are
shown in the oscillograms Fig 31 and are a sufficiently good check on
the performance of the magnetron during the "on" cycle   As it turned
out the choice of pulsed power operation was a good one since no
heating of any of the transformer sections and couplings was observed
even though it was suspected that some of the couplings were not perfect
ly matched

An r f power divider which permitted a three way distribution of
the r f energy was used to drive   components   The r f signal was
divided between the Lecher wire lines and the concentric line velocity
modulator   In order to provide a means for phasing the two pairs of
Lecher wire lines 90° out of phase with respect to one another and at
equal amplitudes of input signal double stub tuners were provided for
each of the Lecher wire inputs   One additional requirement was sepa
ration of the d c circuits of the wire deflection system from the
velocity modulator in order to permit a difference of potential to
exist between both r f systems

A coupler which permitted r f flow while providing d c separation
was placed in series with the concentric line driving the velocity
modulator   The r f power divider and d c separator are shown in the
photograph Fig 32   The output of the velocity modulator was termi-
nated in a type TS 125 10 centimeter wattmeter with a suitable attenu-
ator provided between wattmeter and velocity modulator
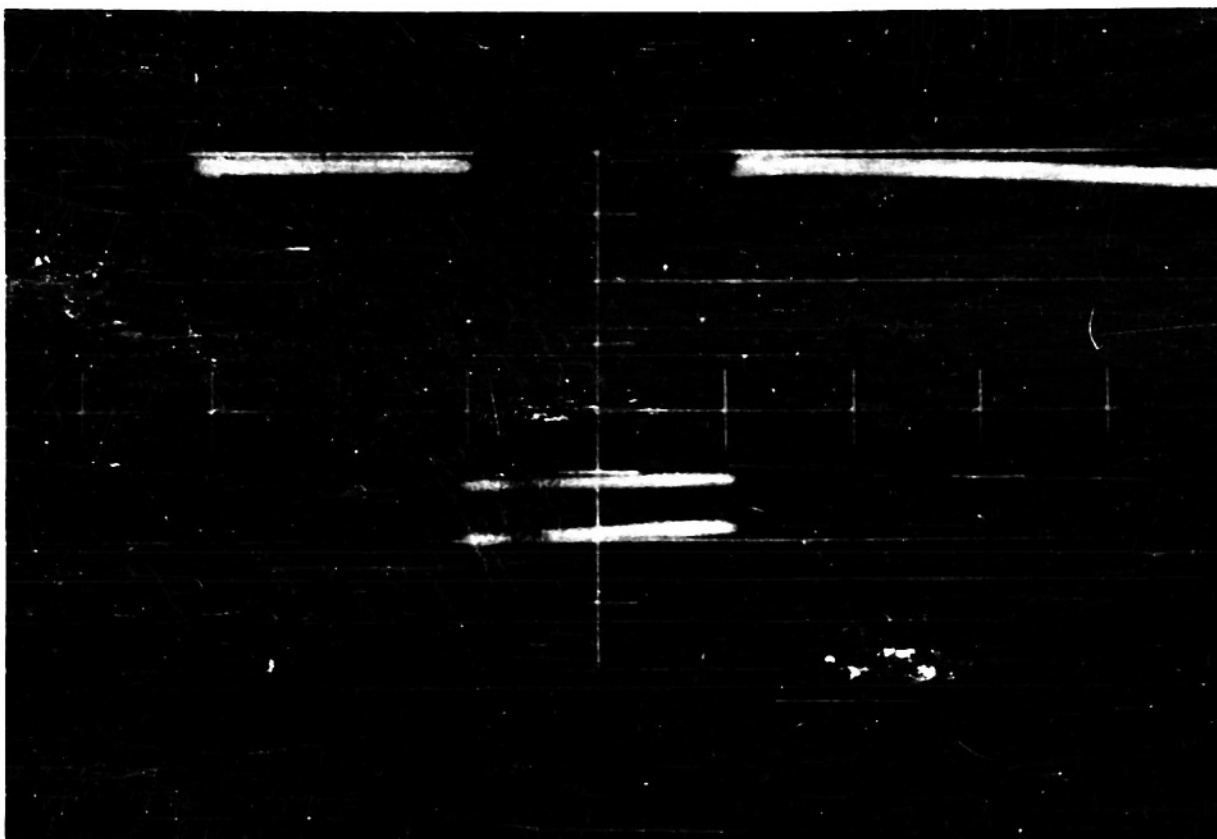
(a)   PULSE DURATION $\tau = 40 \ \mu SEC$:   PPS = 400 PULSES/SEC.
      (UPPER PULSE - VOLTAGE INPUT - LOWER PULSE - R-F OUTPUT)
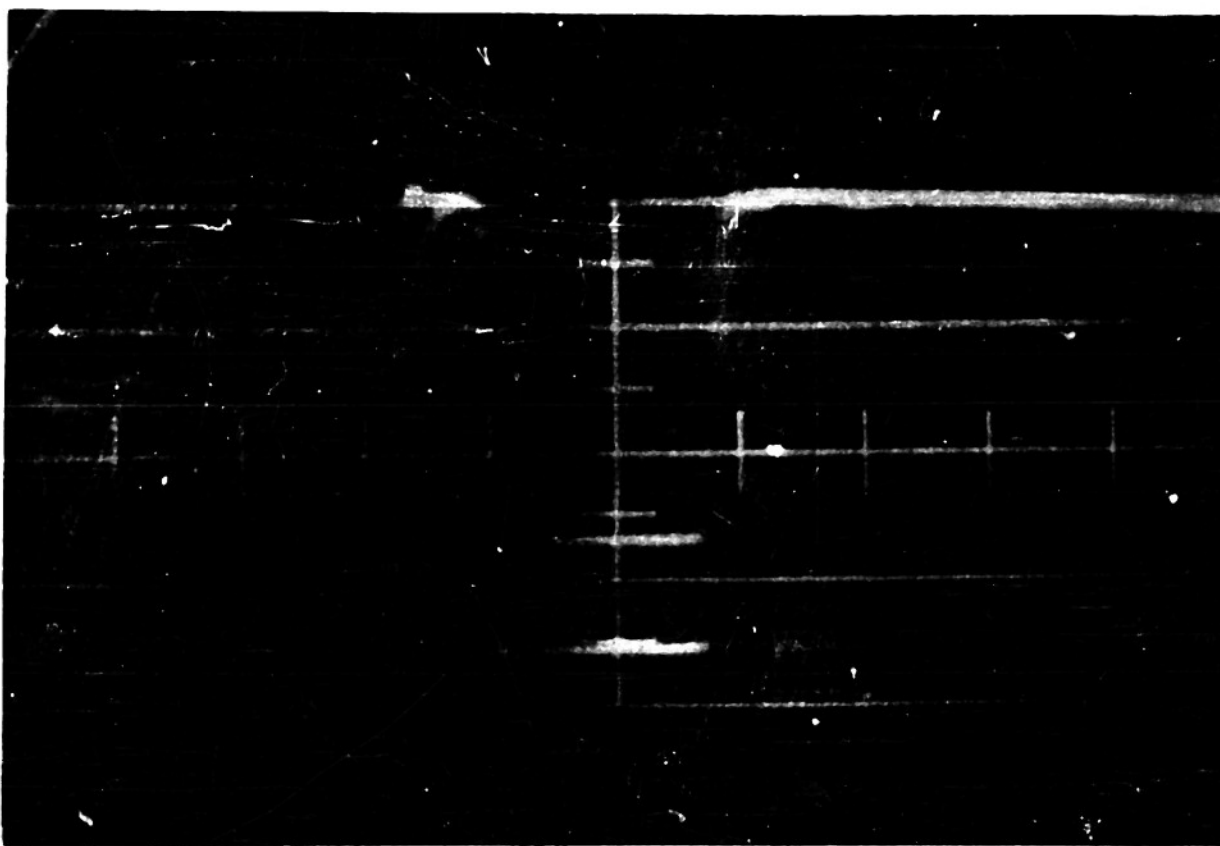
(b) $\tau = 6 \ \mu SEC$;   PPS = 100 PULSES/SEC
      (UPPER PULSE - VOLTAGE INPUT - LOWER PULSE - R-F OUTPUT)
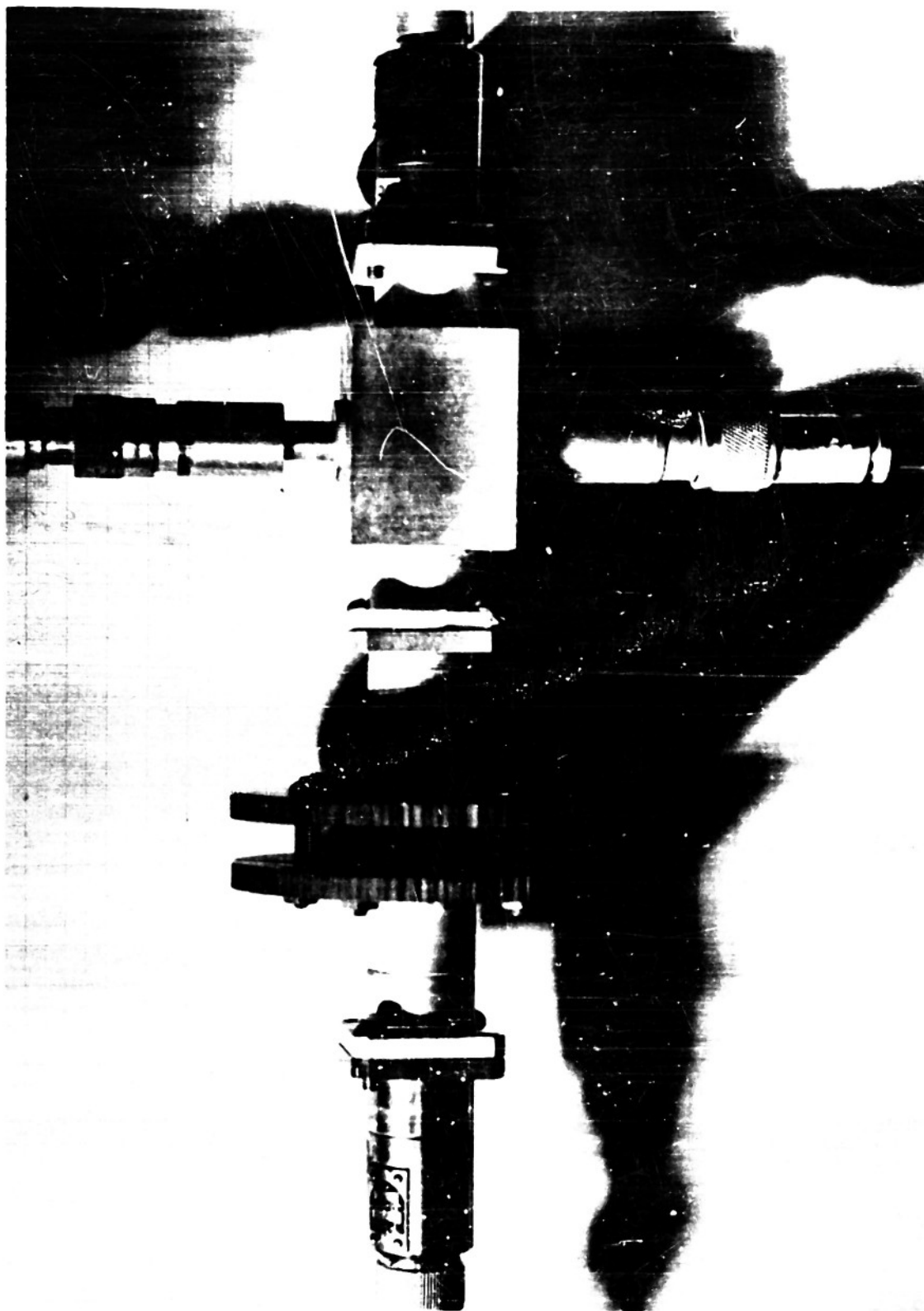   PULSE SHAPE OF R-F GENERATOR OK-60-MAGNETRON

FIGURE 31

FIGURE 32   R-F POWER DIVIDER AND d-c SEPARATOR

3   THE METHOD

The experiments with the velocity modulation source were performed
in the following manner   With the r f system turned off. a beam was
fired through the concentric line power meter and all lens voltage
parameters adjusted so as to provide a small spot on the fluorescent
screen   Deflection corrections due to slight magnetic field displace
ments. misalignment of the first gun etc   were compensated by the d c
electrostatic deflection system provided in the post accelerator so that
the beam would pass through the small square aperture formed t
crossed pairs of Lecher lines
    First the

4 AN IDEALIZED BEAM ANALYZER

From the experimental point of view much could be done to improve the operation and accuracy of the measurements with this deflection-type beam analyzer. Most of the difficulties encountered with the experimental setup were due to the complex output connections

ewing
and
lyzing
ict.re

5. CONCLUSIONS

The velocity-modulation experiments making use of the circularly deflecting analyzer system have proven sufficiently valuable so as to suggest that a series of experimental studies can be carried on with modulated beams from other types of structures as well as further studies on the velocity modulated beam. The oscillograms of the bunched beam presented in the earlier sections show some evidence that space charge effects in the momentary bunch may be quite considerable and should certainly not be neglected as is the case when analytic studies of such beams are usually made.

As was stated, the deflection system which was used for analyzing the beam emerging from the concentric line power meter was not designed for this purpose. The deflection system had been used for measurements of a multipactor beam* and was simply available for the studies presented.

The radial velocity sensitivity was rather small, about 80 volts/mm. Thus, only comparatively large velocity spreads could be measured. However, the velocity sensitivity in the analyzer is primarily a function of the drift length between the two pairs of Lecher wire lines. By making this drift length much greater an increase in sensitivity can be realized which would permit velocity sensitivity to increase as much as a hundred fold. In fact, by carefully refining the structures and increasing the sensitivity it is quite possible to make measurements of velocity spread due to noise in a d-c beam.

As an experimental program making use of an apparatus of the type described earlier in this report, a whole series of experimental studies could be made on modulated beams previously described only by analytical approximate methods.

*[ ] 19(122)-5, Final Report-Millimeter Wave Research, chapter 1, E. W. Ernst and

PART IV
APPENDICES

APPENDIX I

SYMBOLS

a, b	Major and minor axes of an ellipse
d	Diameter of one deflection wire
k	Bunching parameter
s	Distance between two wire pairs
u_a	Instantaneous ac energy component
v, v_o	Electron velocities
x, y	Co-ordinates of deflection
A	An apparatus constant
D	Spacing of the wires in a single wire pair
L	Distance from deflector to screen
P_D	Power fed into the deflector
P_m	Power fed into modulator
R, r	Radii of deflection
S	Distance from modulator to deflector
U, U_o, U_1, U_2	Beam voltages
U_{ac}	ac energy component of the beam
$(U_{ac})_{\Delta R}$ $(\underline{U}_{ac})_{\Delta R}$	Maximum and Minimum ac energy component measured according to ΔR
U_m, U_s, U_S	Characteristic voltages determined by the geometry of the system
U_Δ	$\sqrt{U_s/16} - \sqrt{U_m}$
U_Σ	$\sqrt{U_s/16} + \sqrt{U_m}$
δ	An adjustable phase angle
λ	Free space wave length
μ	Reduced instantaneous ac energy component
ρ_o, ρ_1	Space charge density at modulator and deflector planes respectively
σ	Relative velocity sensitivity

SYMBOLS
(contd)

σ_{Fast} σ_{Slow}	Relative velocity sensitivity along the fast and the slow axis
ξ $\cdot$	Coordinates along the major and minor axes of an ellipse
φ	Phase angle along the beam
φ_0. φ_1	Phase angle of departure and arrival
$\dot{\varphi_0}$ $\dot{\varphi_1}$	Phase angle at which bunches occur
$\psi(U)$	Coupling function of the modulator into the beam
θ	Geometrical deflection angle Azimuthal angle
$\Delta\theta'$	Bunch separation angle
Φ. Φ_0 Φ_1	Transit angles

APPENDIX II

It may be pointed out that Eq. (52) takes care of the ac-velocity jump in the post-acceleration gap* because the energy concept was used throughout

$$k = 1.285 \cdot 10^3 \cdot \hat{r}_m \frac{\psi(U_1)}{(U_1 + U_2)^{3/2}} \tag{52}$$

Thus, for constant power delivered to the modulator, k should remain constant if the sum $U_1 + U_2$ and $\psi(U_1)$ remain constant, whatever the post-acceleration voltage U_2 may be. Looking at the coupling function $\psi(U_1)$ as presented in Fig. 14, it may be seen that $\psi(U_1)$ remains almost constant for a wide variation of U_1 e.g. from 1600 volts to 3000 volts. This fact can be used to check experimentally the constancy of k with different post-acceleration voltages U_2 only if the total beam voltage $U_1 + U_2$ remains constant.

For this purpose an experiment was performed in which the power delivered to the modulator was kept constant at 11.4 watts, the injector voltage U_1 was raised stepwise and the post-acceleration voltage accordingly lowered in order to keep $U_1 + U_2$ constant. Photographs were taken in five positions to measure k according to an observable bunch-separation angle $\Delta\vartheta^*$.

The values chosen are given in Table IA. The bunching parameter k is computed according to Eq. (52) and from this with Eq. (45) or Fig. 18, the value of the bunch separation angle $\Delta\vartheta^*$ is determined. In the last column the expected ac-velocity jump is computed, which would satisfy Eq. (52). The ac-velocity component before and after the jump $[(v_{ac})_0; (v_{ac})_1]$ are related to each other by:

$$\frac{(v_{ac})_1}{(v_{ac})_0} = \sqrt{\frac{U_1}{U_1 + U_2}} \tag{1A}$$

TABLE IA

Fig. No.	U_1	U_2	$U_1 + U_2$	$\psi(U_1)$	k	$(\Delta\theta^*)_{Theor}$	$\frac{(v_{ac})_1}{(v_{ac})_0}$
A1	1580	1930	3560	70.5	1.47	29°	0.666
A2	1780	1750	3530	72.5	1.54	35°	0.710
A3	1980	1500	3480	73.0	1.59	40°	0.755
A4	2190	1250	3440	74.0	1.64	44°	0.799
A5	2400	1000	3400	74.0	1.66	46°	0.840

* See: Ping King Tien and Lester M. Field. *Space-Charge Waves in an Accelerated Electron Stream for Amplification of Microwave Signals.* Proceedings of the Institute of Radio Engineers. Volume 40. Appendix I. pp 688-695.

It may be noted that the total beam voltage was not kept constant during the experiment which causes a slight increase in k. The reason for the lack of constancy in the total beam voltage is that a change in U_1 changes the exit phase of the modulated beam after passing through the modulator and has to be compensated by a change of the drift space if one desires to place the bunching action along the sensitive slow axis i e keep it on a constant arrival phase angle

The pictures taken are presented in Figs Al to A5 The expected bunch separation angle $\Delta\theta^\circ$ is indicated on the pictures The agreement can be considered as good
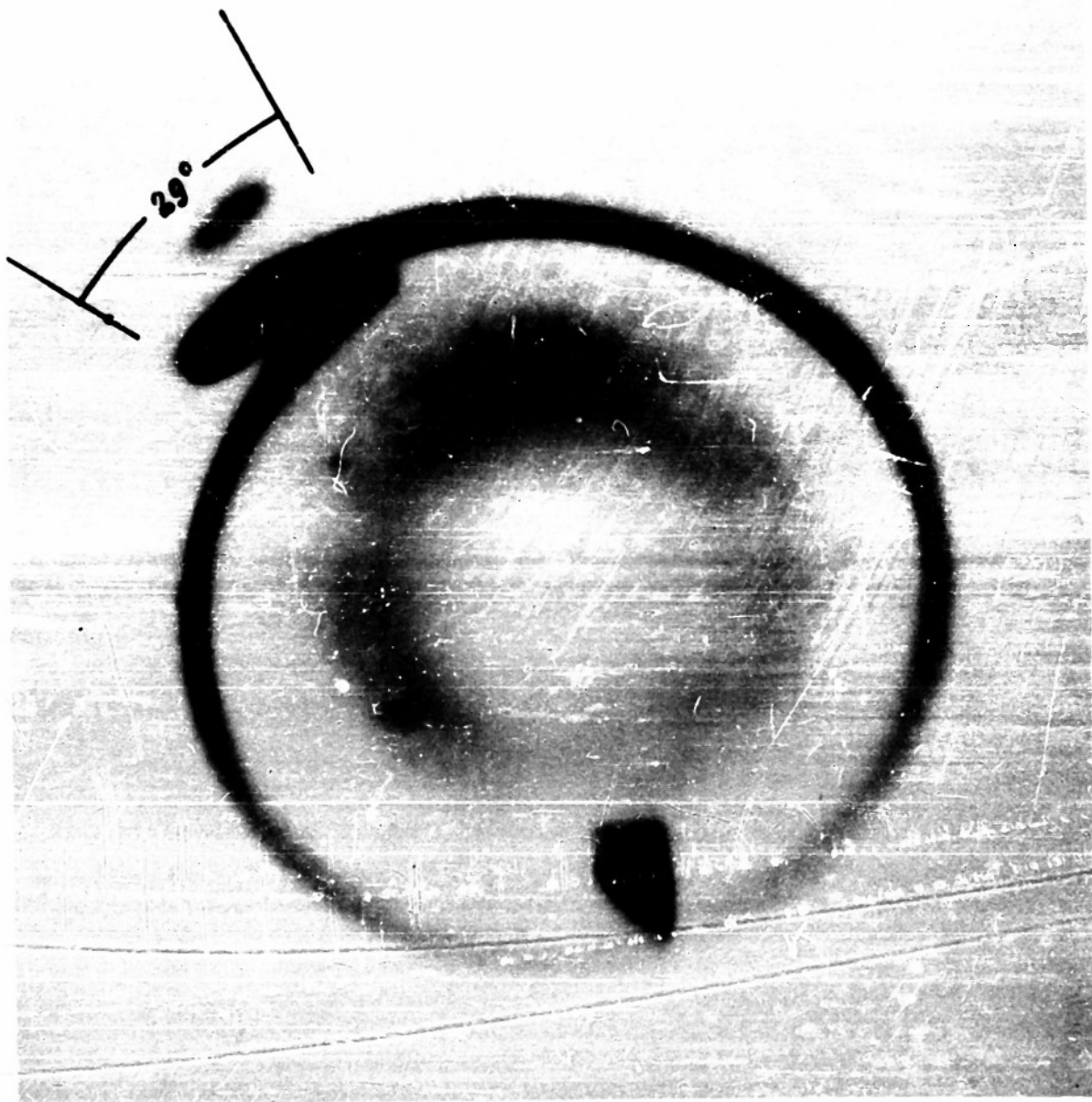
FIGURE A1

U$_1$ = 1580 VOLTS   K = 1.47

U$_2$ = 1980 VOLTS $\Delta\theta^{\circ}$ = 29°
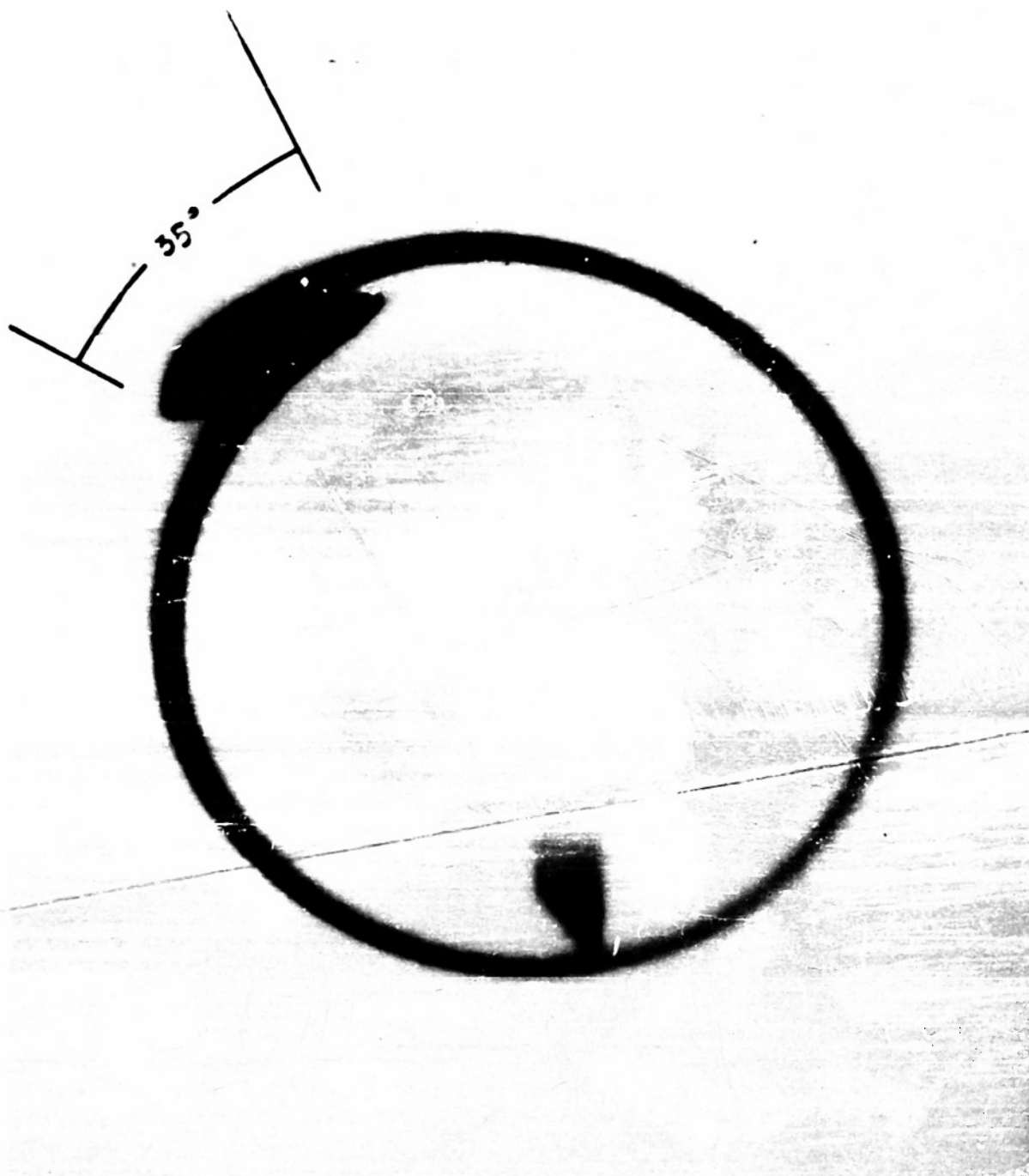
U$_1$ + U$_2$ = 3560 VOLTS

FIGURE A2

U_1 = 1780 VOLTS   K = 1.54

U_2 = 1750 VOLTS $\Delta\theta^{\circ}$ = 35°
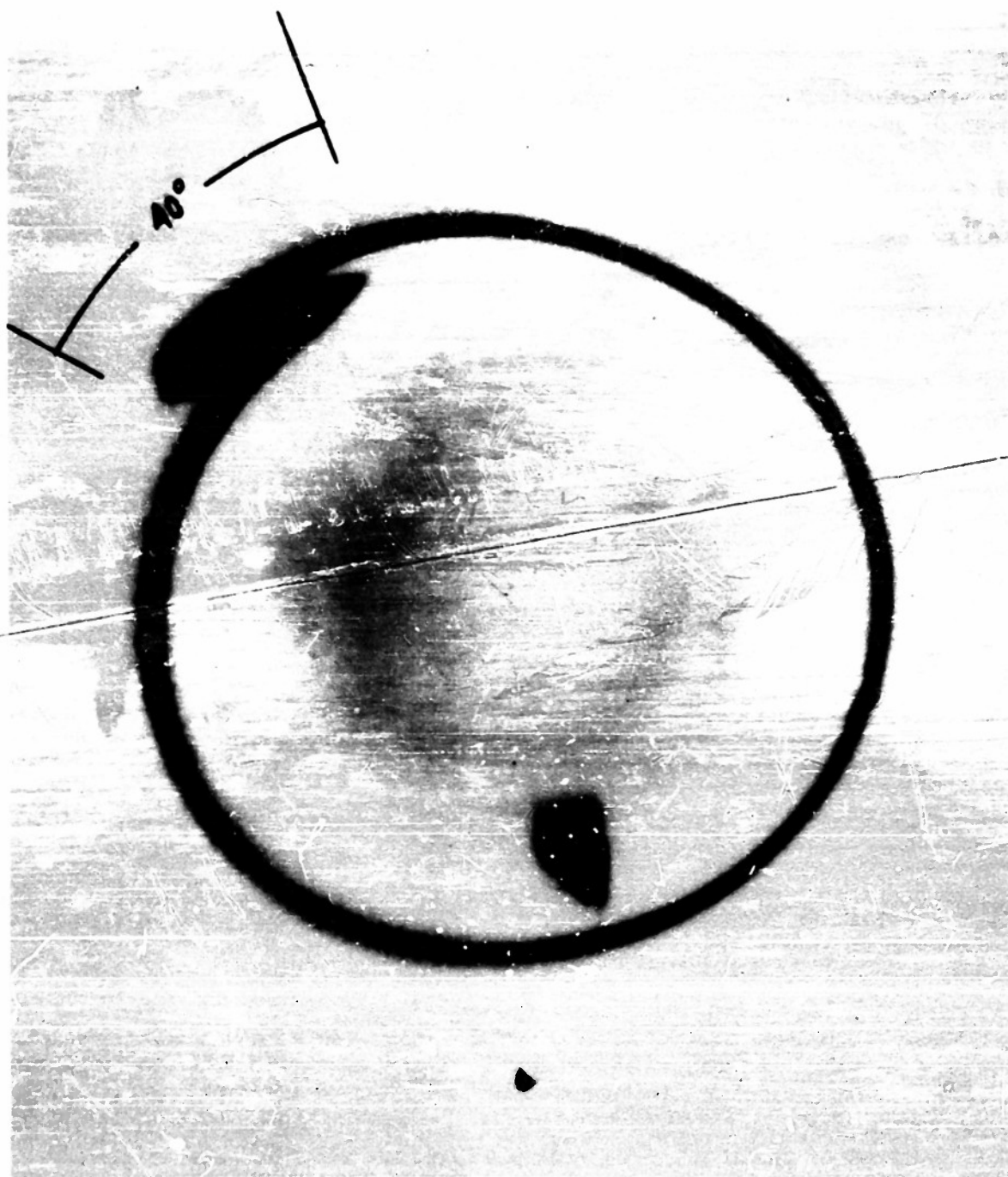
U_1 + U_2 = 3530 VOLTS

FIGURE A3

U_1 = 1980 VOLTS K = 1.59

U_2 = 1500 VOLTS $\Delta\theta^*$ = 40°

$U_1 + U_2$ = 3480 VOLTS

FIGURE A4

U_1 = 2190 VOLTS   K = 1.64

U_2 = 1250 VOLTS $\Delta\theta^*$ = 44°

U_1 + U_2 = 3440 VOLTS

FIGURE A5

$U_1 = 2400$ VOLTS $K = 1.66$

$U_2 = 1000$ VOLTS $\Delta\theta^* = 46°$

$U_1 + U_2 = 3400$ VOLTS

14 Ramo and Whinnery   *Fields and Waves in Modern Radio*   Wiley New York 1944.
    Chapter 9.

15 Rudenberg, H G   *Deflection Sensitivity of Parallel Wire Lines in Cathode Ray
    Oscillographs*. J Appl Phys   Volume 16   May 1945   p 279

16 Smith, S T , Talbot, R V and Smith, C H , Jr   *Cathode Ray Tube for Recording
    High-Speed Transients*. Proceedings of the Institute of Radio Engineers, Volume
    40   March 1952   pp 297-302